Thesis for doctoral degree (Ph.D.) 2009

In Vivo Imaging of the Cannabinoid CB_1 Receptor using Positron Emission Tomography

Garth Terry

Karolinska Institutet

Thesis for doctoral degree (Ph.D.) 2009

In Vivo Imaging of the Cannabinoid CB_1 Receptor using Positron Emission Tomography

Garth Terry

Thesis for doctoral degree (Ph.D.)
2009

In Vivo Imaging of the Cannabinoid CB_1 Receptor using Positron Emission Tomography

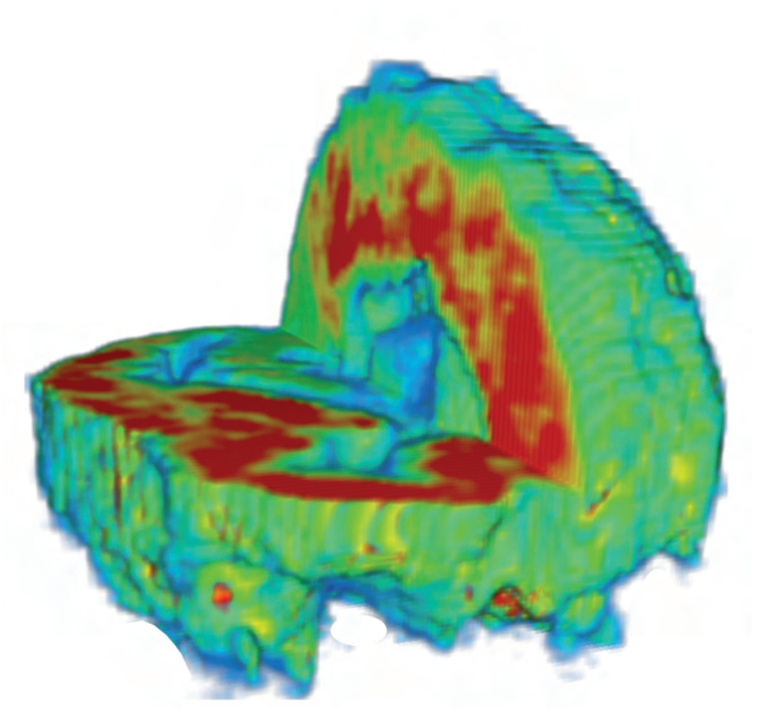

Garth Terry

Karolinska Institutet

From THE DEPARTMENT OF CLINICAL NEUROSCIENCE
Karolinska Institutet, Stockholm, Sweden

IN VIVO IMAGING OF THE CANNABINOID CB_1 RECEPTOR USING POSITRON EMISSION TOMOGRAPHY

Garth Terry

Stockholm 2009

Cover: 3D volume rendering of [^{18}F]FMPEP-d_2 as distribution volume, depicting CB_1 receptor density and distribution in human brain.

Published by Karolinska Institutet.
Printed by University Service US-AB, Stockholm.

ISBN 978-91-7409-677-4

ABSTRACT

The actions of marijuana (cannabis) are mediated by receptors (primarily the cannabinoid CB_1 receptor) that have unusually high density and wide distribution in brain. In addition to mediating the effects of exogenous drugs like cannabis, these receptors also receive signals from endogenous cannabinoids (endocannabinoids), which modulate the release of several other neurotransmitters. Since abnormalities of cannabinoid receptors and endocannabinoid transmission have been hypothesized to underlie disorders of the brain (*e.g.,* memory impairment, schizophrenia, and seizures), this neurotransmitter system has been an active target for development of drug therapies and of biomarkers to measure its *in vivo* function. Positron emission tomography (PET) can image the distribution of receptors in the body, is a powerful tool for drug development, and can quantify the receptor as a biomarker to assess pathophysiology. The purpose of this thesis was to evaluate several candidate PET radioligands for their relative ability to quantify CB_1 receptors in the living brain of animals and humans.

We first assessed [^{11}C]MePPEP as a PET radioligand through studies in rodents. Wild-type and genetically modified mice were used to determine that [^{11}C]MePPEP is not a substrate for the P-glycoprotein efflux transporter and that the majority (about two-thirds) of its binding in brain is specific to the CB_1 receptor. Pharmacologically active doses of CB_1 agonists had no effect on [^{11}C]MePPEP in rats, which suggests a large CB_1 receptor reserve. Pharmacokinetic modeling of CB_1 receptors using brain radioactivity and measurements of radioligand in arterial plasma yielded stable measures after 70 minutes of scanning. The results suggest that [^{11}C]MePPEP might be successful in humans, although competition studies with endocannabinoids would not be possible, and radiometabolites might cause consistent overestimation of CB_1 receptor density.

Second, we examined [^{11}C]MePPEP in healthy human subjects using the "gold standard" of compartmental modeling to quantify receptor density in brain. [^{11}C]MePPEP had high uptake in brain, could be imaged for 210 minutes, and could quantify CB_1 receptors within about 60 minutes of scanning. However, the accuracy and precision of the pharmacokinetic modeling hinged upon the accuracy of radioligand measurements in arterial plasma. A radioligand with a longer radioactive half-life, such as from ^{18}F, would be expected to provide superior measurements in arterial plasma.

We then evaluated several ^{18}F-radiolabeled analogues of MePPEP in monkey. [^{18}F]FMPEP-d_2 was selected for study in human due to its superior uptake in brain compared to [^{18}F]FEPEP, and reduced uptake of radioactivity in bone compared to [^{18}F]FMPEP. In humans, [^{18}F]FMPEP-d_2 could image and quantify CB_1 receptors with better accuracy and precision compared to that of [^{11}C]MePPEP. As suspected, the accuracy in measuring radioligand in arterial plasma was the critical improvement needed in the pharmacokinetic modeling.

Finally, we examined the biodistribution and radiation dosimetry estimates in human for [^{11}C]MePPEP and [^{18}F]FMPEP-d_2. Both radioligands had high uptake in brain, liver, and lungs, and both had significant uptake of radioactivity in bone marrow, but not in bone. Regardless, both radioligands have an effective dose similar to that of other clinically used PET radioligands.

In conclusion, we have shown that both [^{11}C]MePPEP and [^{18}F]FMPEP-d_2 can quantify CB_1 receptors in brain. However, [^{18}F]FMPEP-d_2 is superior to [^{11}C]MePPEP because it has greater precision and accuracy. Thus, [^{18}F]FMPEP-d_2 is a promising PET radioligand to measure CB_1 receptors *in vivo*, and can now be used to explore the role of this receptor in human health and disease.

LIST OF PUBLICATIONS

I. Terry GE, Liow JS, Chernet E, Zoghbi SS, Phebus L, Felder CC, Tauscher J, Schaus JM, Pike VW, Halldin C, Innis RB. (2008) Positron emission tomography imaging using an inverse agonist radioligand to assess cannabinoid CB_1 receptors in rodents. *NeuroImage* 41:690-698.

II. Terry GE, Liow JS, Zoghbi SS, Hirvonen J, Farris AG, Lerner A, Tauscher JT, Schaus JM, Phebus L, Felder CC, Morse CL, Hong JS, Pike VW, Halldin C, Innis RB. (2009) Quantitation of cannabinoid CB_1 receptors in healthy human brain using positron emission tomography and an inverse agonist radioligand. *NeuroImage* 48:362-370.

III. Terry GE, Hirvonen J, Liow JS, Zoghbi SS, Gladding R, Tauscher JT, Schaus JM, Phebus L, Felder CC, Morse CL, Donohue SR, Pike VW, Halldin C, Innis RB. Imaging and quantitation of cannabinoid CB_1 receptors in human and monkey brain using ^{18}F-labeled inverse agonist radioligands. *Journal of Nuclear Medicine*. In press.

IV. Terry GE, Hirvonen J, Liow JS, Seneca N, Tauscher JT, Schaus JM, Phebus L, Felder CC, Morse CL, Pike VW, Halldin C, Innis RB. Biodistribution and dosimetry in humans of two inverse agonists to image cannabinoid CB_1 receptors using positron emission tomography. *European Journal of Nuclear Medicine and Molecular Imaging*. Submitted.

CONTENTS

LIST OF ABBREVIATIONS

AAL	Automated anatomical labeling
ABHD4	abhydrolase domain-containing protein
2-AG	2-arachidonoyl glycerol
AIC	Akaike Information Criterion
AIDS	Acquired immunodeficiency syndrome
AM404	An endocannabinoid transporter inhibitor
ATLAS	Advanced Technology Laboratory Animal Scanner
AUC	Area under the curve
B_{max}	Binding maximum (*i.e.*, total receptor density)
cAMP	3'-5'-cyclic adenosine monophosphate
CB_1	Cannabinoid subtype 1
CB_2	Cannabinoid subtype 2
CB_3	Cannabinoid subtype 3
CNR1	Gene encoding cannabinoid subtype 1 receptor
CNS	Central nervous system
C_{NS}	Concentration non-specifically bound
C_P	Concentration in plasma
C_S	Concentration specifically bound
CP-55,940	A non-classical cannabinoid agonist
C_T	Concentration in tissue
COX-2	Cyclooxygenase type 2
DAGLα, DAGLβ	diacyglycerol lipase alpha and beta
D_2	Dopamine subtype 2
ET	Endocannabinoid transporter
FAAH	Fatty acid amide hydrolase
FDA	Food and Drug Administration
FDG	Fluorodeoxyglucose
GABA	γ-aminobutyric acid
GPCR	G protein-coupled receptor
GPR55	G protein-coupled receptor 55
GTP	Guanosine-5'-triphosphate
Hemoglobin A1c	Glycosylated hemoglobin
HIV	Human immunodeficiency virus
HDL	High density lipoprotein
HPLC	High-performance liquid chromatography
HRRT	High resolution research tomography
ICC	Intraclass correlation coefficient
ICRP	International Commission on Radiological Protection
IV	Intravenous
K_1, k_2, k_3, k_4	Kinetic parameters (*i.e.*, rate constants)
keV	Kiloelectron volts
KI	Karolinska Institutet
LTD	Long-term depression
LTP	Long-term potentiation

MAGL	Monoacylglycerol lipase
MAP	mitogen activated protein
MIB	Molecular Imaging Branch
MDR1	Multidrug resistance gene 1 (encodes P-gp)
MNI	Montreal Neurological Institute
MRI	Magnetic resonance image
mRNA	Messenger ribonucleic acid
MSC	Model selection criteria
NAAA	*N*-acylethanolamine acid amidase
NAPE-PLD	*N*-acyl-phosphatidylethanolamine-selective phospholipase D
NIH	National Institutes of Health
NIMH	National Institute of Mental Health
NSAID	Non-steroidal anti-inflammatory drug
OLINDA	Organ level internal dose assessment
PBR	Peripheral benzodiazepine receptor
PET	Positron emission tomography
P-gp	P-glycoprotein (an efflux transporter)
PKA	Protein kinase A
PPAR	Peroxisome proliferator-activated receptor
PTPN22	Protein tyrosine phosphotase, non-receptor type 22
SD	Standard deviation
SE	Standard error
SUV	Standardized uptake value
Δ^9-THC	Δ^9-tetrahydrocannabinol
TRPA1	Transient receptor potential ankyrin 1 (a cation channel)
TRPV1	Transient receptor potential vanilloid 1 (a cation channel)
TSPO	Translocator protein (18kDa)
URB597	A FAAH inhibitor
V_T	Total distribution volume
WIN 55,212-2	An aminoalkylindole cannabinoid agonist

INTRODUCTION

Cannabis has been used for its medical and psychotropic effects for thousands of years, and remains the most commonly used illegal drug in the world today[1]. However, the molecular underpinnings that mediate the effects of cannabis and its principle component, Δ^9-tetrahydrocannabinol (Δ^9-THC), have only recently been uncovered. Cannabinoid receptors are found throughout the brain, the immune system, and various organs, and receive signals from endogenous cannabinoids (endocannabinoids), and serendipitously from Δ^9-THC. In the brain, endocannabinoids function to modulate other neurotransmitters. Therefore, perturbations to the endocannabinoid system can either cause, or be the result of, disrupted brain function (*e.g.* memory impairment) or neuropsychiatric disease (*e.g.* schizophrenia or seizures). Hence, cannabinoid receptors are an attractive target for pharmacotherapy development and biomarker research to enhance our understanding of these diseases and their treatment. Positron emission tomography (PET) can image the distribution of receptors in the body, is a powerful tool for drug development, and can quantify the receptor as a biomarker to assess pathophysiology.

ENDOCANNABINOID SYSTEM

Cannabinoid receptors are named for their historical association to the cannabinoid compounds that bind to them, which themselves are derived from genus of *Cannabis* plants. The endocannabinoid system refers to these receptors, their endogenous ligands, and associated enzymes, transporters, and carriers that exist in the body and function in an integrated manner. In the brain, the endocannabinoid system inhibits the actions of other neurotransmitters systems and, in effect, buffers excitatory and inhibitory signaling.

Cannabinoid receptors

Cannabinoid receptors are G protein-coupled receptors (GPCR), which are seven-transmembrane domain proteins that mediate intracellular actions through guanosine-5'-triphosphate (GTP) activated mechanisms[2]. When stimulated, the receptor signals intracellular proteins that initiate a cascade of events altering cellular function. The resulting changes vary by cell type, and can include increased or decreased activation of many other proteins, opening or closing ion channels, and regulation of genetic transcription[3]. The net effect of these changes typically has consequences on intercellular signaling and connectivity, metabolism, and inflammation, to name a few.

The first cannabinoid receptor discovered, named CB_1, is primarily found in the brain and mediates the psychotropic effects of cannabis. This receptor has come to prominence not only for its association with cannabis, but also for its involvement in a multitude of diseases and as a target for pharmacotherapy. The second receptor discovered, named CB_2, is primarily associated with the immune system. There is only 48% amino acid homology between CB_1 and CB_2 receptors, however their transmembrane domain share 68% amino acid homology[4]. Since most agonists activate

both CB_1 and CB_2 receptors, it is not surprising that the active binding site resides in the transmembrane domain[5,6]. However other cannabinoid effects have been observed when agonists are administered to rodents after CB_1 and CB_2 receptors are blocked, suggesting the existence of other cannabinoid receptors. Recently, GPR55 has been proposed as a CB_3 receptor, since it has affinity for THC and endocannabinoids[6]. Likewise, members of the transient receptor potential family of ion channels (TRPV1, TRPA1, and others) are sensitive to cannabinoid agonists, although they are not considered part of the cannabinoid family at present[2].

The CB_1 receptor can be found in sea squirts, fish, reptiles, and all mammals, and likely co-evolved with the rest of the endocannabinoid system[8-10]. This suggests that the endocannabinoid system in mammals is evolutionarily ancient[11]. It may be surprising, therefore, that genetic deletion of CB_1 receptors in mice is not lethal, although it may cause a reduction in lifespan. These CB_1 receptor knockout mice demonstrate generally reduced activity, described as hypoactivity, hypolocomotion, hypophagia, and hypoalgesia[12]; interestingly, these mice also demonstrate reduced signs of addiction to drugs of abuse[13]. In human the CB_1 receptor is encoded by the *CNR1* gene on chromosome 6 q14-q15, and is expressed by a single exon[14]. An uncommon splice variant of the mRNA has been discovered, but it is unclear if this leads to functionally distinct CB_{1a} and CB_{1b} receptors[15]. Several single nucleotide polymorphisms of *CNR1* have been associated with psychiatric[16] and metabolic[17] diseases. Across mouse, rat, and human there is ≥97% amino acid homology[18], suggesting the rodents are appropriate models for studying CB_1 receptors.

CB_1 receptors are found throughout the human body, with the highest concentration in the brain. They are believed to be the highest density GPCR found within the brain, estimated from the receptor density (B_{max}) measured in mice (1.81 pmol/mg)[19] and rat cerebella (1752 fmol/mg protein)[20], at concentrations near that of amino acid neurotransmitters. CB_1 receptors are found in nearly every brain structure, with particularly high densities in basal ganglia, hippocampus, cerebral cortex, and the molecular layer of the cerebellum. They are expressed in lower densities in thalamus, pons, and medulla, and essentially absent in white matter[21,22]. While CB_1 receptors are mostly expressed on neurons, they are also found on astrocytes, oligodendrocytes, and microglia[23]. Outside of the brain, CB_1 receptors are found in the liver, gastrointestinal tract, peripheral neurons, and heart, as well as on adipocytes, myocytes, and sperm in addition to many other tissues[24]. The function of CB_1 receptors outside of the brain may vary by tissue, and is beyond the scope of this thesis.

Cannabinoid ligands

The *sine qua non* cannabinoid is Δ^9-tetrahydrocannabinol (Δ^9-THC) (Fig. 1). Even though the active ingredient in opioids, morphine, was isolated by 1804, it was not until 1964 that Raphael Macholoum was able to isolate the main psychoactive ingredient in cannabis, Δ^9-THC[25]. Due to its high lipophilicity and its multiple wide-

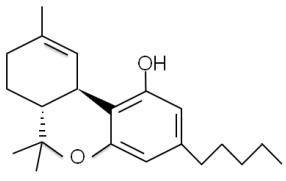

Figure 1. Structure of Δ^9-THC

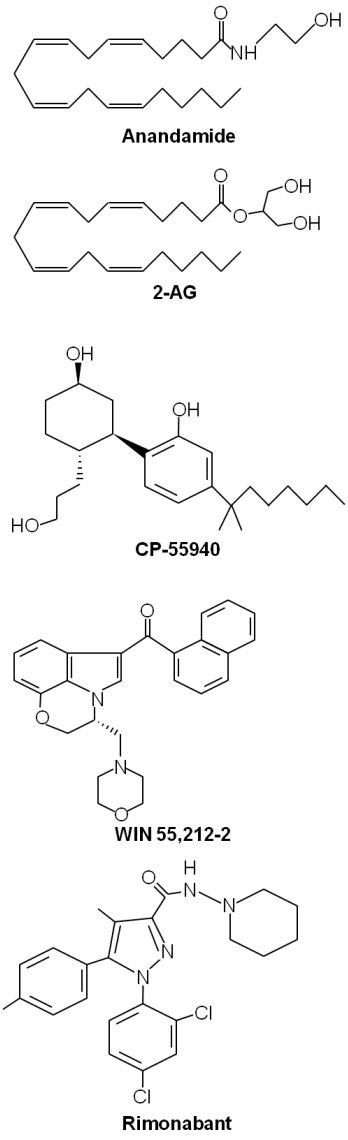

Figure 2. Structures of two endocannabinoids (anandamide, 2-AG), two cannabinoid agonists (CP-55940, WIN 55,212-2), and a CB_1 receptor-selective inverse agonist (rimonabant)

ranging effects, Δ^9-THC was believed to act primarily by disturbing the plasma membranes of neurons. Shortly after the structure of Δ^9-THC was elucidated, it was demonstrated that cannabinoid stereoisomers had differential effects, suggesting that there was a specific protein receptor[26,27]. It was another 26 years before that receptor was discovered. Currently there are more than 60 recognized cannabinoids derived from plants, which are termed phytocannabinoids.

Discovery and cloning of the CB_1 receptor[28] prompted the search for the endogenous ligand(s) that activate it. Arachadonoyl-ethanolamine was the first of such to be identified[29], and was nicknamed anandamide, derived from the Sanskrit word "ananda" meaning bliss (Fig. 2). This discovery was quickly followed by the identification of 2-arachidonoyl glycerol (2-AG)[30]. Several other arachidonic acid derivatives have been identified as endocannabinoids, including *N*-arachidonoyl-dopamine[31], 2-arachidonyl glyceryl ether (noladin ether)[32], and *O*-arachidonoyl ethanolamine (virodhamine)[33], bringing the count to about 12 recognized compounds[34]. Anandamide and 2-AG are the most heavily studied endocannabinods, and are likely the most relevant ones to the endocannabinoid system in the brain. Acting alone they can behave as partial agonists, triggering different subsets of alpha proteins found coupled to the cannabinoid receptors[35,36], but working together they can achieve the full agonist response; this functional selectivity likely increases the specificity of their effects *in vivo*.

Elucidation of the structure of cannabinoids afforded organic chemists the means to create analogues that have higher binding affinity (increased potency) and higher selectivity compared to the naturally occurring cannabinoids. There are six main classes of cannabinoids: classical cannabinoids (*e.g.*, Δ^9-THC), non-classical cannabinoids (*e.g.*, CP-55,940), hybrid cannabinoids, aminoalkylindoles (*e.g.*, WIN 55,212-2), diarylpyrazoles (*e.g.*, rimonabant), endocannabinoids (*e.g.*, anandamide)[37]. The first three are agonists and are essentially comprised of Δ^9-THC, its natural and synthetic

analogs. The majority of these compounds are non-selective for CB_1 and CB_2 receptors, although many of them are stereoselective. Notably, CP-55,940 has nearly 45 times higher potency for CB_1 receptors than Δ^9-THC, and higher efficacy in many *in vitro* assays[38]. WIN 55,212-2, an aminoalkylindole, is structurally distinct from the classical cannabinoids, as it was independently discovered as a potential non-steroidal anti-inflammatory drug (NSAID)[39], and is less lipophilic than other cannabinoid agonists.

Rimonabant was the first inverse agonist to offer significant CB_1 receptor selectivity[40]. CB_1 receptors have intrinsic activity, meaning that they can initiate intracellular signaling in the absence of an agonist[35]. Therefore, CB_1 receptors are sensitive to inverse agonism; that is, inverse agonists inhibit the intrinsic activity of the receptor and cause an apparent reversal of intracellular activity[41]. However, this mechanism has been debated against experimental evidence which suggests constituitive activity of endocannabinoids tonically stimulate CB_1 receptors, and so this phenomenon is not completely understood[42]. Nevertheless, compounds such as rimonabant demonstrate inverse agonism and are able to block endogenous signaling.

Neurotransmission of endocannabinoids at the CB_1 receptor

A major role of the CB_1 receptors is their action on neuromodulation in the brain. When a presynaptic neuron is stimulated by excitatory signals, calcium channels located near the synaptic membrane are triggered to open, letting calcium into the neuron (Fig. 3a). The increased concentration of calcium stimulates the mobilization of vesicles containing neurotransmitters, which then fuse with the synaptic membrane. The presynaptic neuron releases neurotransmitter such as GABA, glutamate, or dopamine,

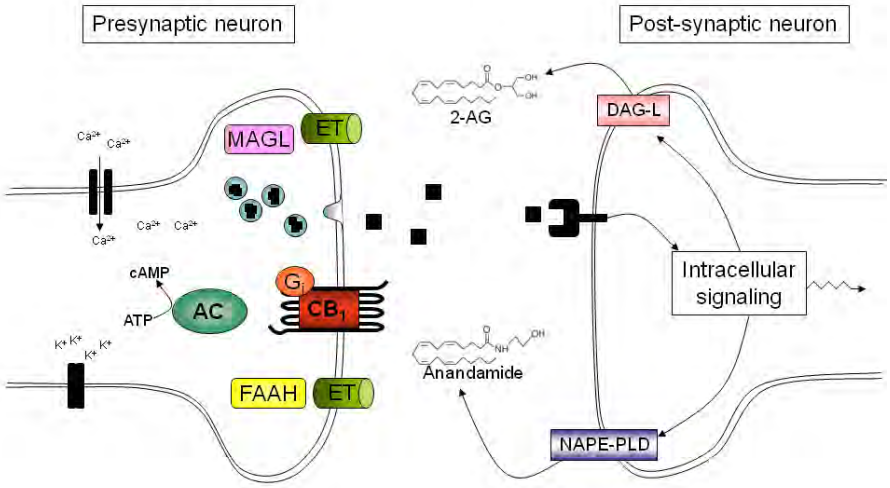

Figure 3a. Endocannabinoid release into the synapse. Entry of calcium into the presynaptic neuron triggers the release of neurotransmitters (■) such as GABA, glutamate, or dopamine from storage vesicles into the synapse. After the neurotransmitter binds to its native receptor, intracellular signals result including the stimulation of NAPE-PLD to synthesize anandamide, and/or the stimulation of DAG-L to synthesize 2-AG. The endocannabinoids are released into the synapse and travel back toward the presynaptic neuron in a process termed retrograde neurotransmission.

which travels to its native receptor on the post-synaptic membrane. Synthetic enzymes are stimulated to create and release endocannabinoids, such as anandamide. The endocannabinoid then travels back to the presynaptic neuron and bind with CB_1 receptors, a process termed retrograde neurotransmission. Typically, the endocannabinoid signal causes the inhibition of adenylyl cyclase which in turn causes the calcium channels to close, decrease the amount of primary neurotransmitter released from the presynaptic neuron.

In contrast to most vesicle stored neurotransmitters, endocannabinoids are produced on demand directly from membrane-bound phospholipids. The synthetic enzymes of endocannabinoids are located in the synaptic membrane, and are likely part of a complex and redundant system of pathways. In the case of anandamide, *N*-acyl-phosphatidylethanolamine-selective phospholipase D (NAPE-PLD)[43], abhydrolase domain-containing protein (ABHD4)[44], and protein tyrosine phosphotase, non-receptor type 22 (PTPN22)[45] have been described as relevant synthetic enzymes. 2-AG is known to be synthesized by diacylglycerol lipase alpha and beta (DAGLα and DAGLβ)[46]. These enzymes are likely stimulated by the increase of intracellular calcium or depolarization of the postsynaptic neuron.

Endocannabinoids translate their effect through cannabinoid receptors primarily by G_i and G_o subtype proteins (Fig. 3b). These in turn inhibit adenylyl cyclase, decreasing the production of cAMP, which reduces further activation of other intracellular proteins, such as protein kinase A (PKA)[3]. These signals have the effect of closing calcium channels, which reduces the influx of calcium and the mobilization of vesicles containing neurotransmitters. Cannabinoid receptors also stimulate G protein activated

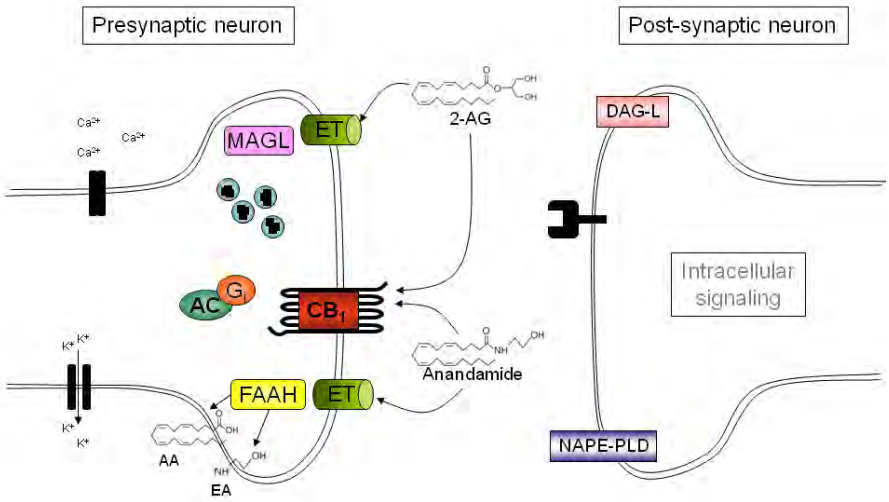

Figure 3b. Endocannabinoid signaling and degradation. After traveling from the post-synaptic neuron to the pre-synaptic neuron, the endocannabinoid (anandamide, 2-AG) may bind with the CB_1 receptor. The resulting effects include inhibition of adenylyl cyclase (AC) by the inhibitory G protein (G_i), closing of the calcium channel which inhibits neurotransmitter (■) release, and opening of the G protein-coupled inwardly rectifying potassium channel (GIRK). Excess anandamide may be taken up by the endocannabinoid transporter (ET) and hydrolyzed by fatty acid amide hydrolase (FAAH) into arachadonic acid (AA) and ethanolamide (EA), which are recycled by the synaptic membrane. Excess 2-AG undergoes a similar process, and is degraded by monoglycerol lipase (MAGL).

inward rectifying potassium channels, which have the added effect of repolarizing the neuron, further inhibiting neurotransmitter release. In some cells, CB_1 receptors are coupled to G_s proteins, which stimulate adenylyl cyclase, while in others they mediate the rapid actions of glucocorticoids in the brain[47], and cytokine signaling in the brain[48]. Other effects of CB_1 stimulation, such as activation of mitogen activated protein (MAP) kinase and peroxisome proliferator-activated receptor (PPAR) gamma leading to gene expression[49], are still being uncovered and understood by researchers.

Neuromodulation mediated by the endocannabinoid system has effects on synaptic plasticity, learning, and memory. By inhibiting the excitatory or inhibitory signal that ultimately gets transmitted, endocannabinoids can facilitate the long-term potentiation (LTP) or long-term depression (LTD) between two neurons[50]. Both LTP and LTD contribute to the formation and storage of memory, and underlie the process of learning. The process of learning and memory formation likely depend on the timing and location of endocannabinoid release, which permits the extinction of previous memories[51]. Therefore, global stimulation of CB_1 receptors, as from cannabis, interrupts the local formation of LTP and LTD and delays learning and memory.

All neurotransmitter systems have a mechanism for neurotransmitter degradation, and the endocannabinoid system is no exception. Indirect evidence supports the presence of an endocannabinoid transporter on post-synaptic membranes, however no protein structure has been elucidated to confirm its existence[52]. Catabolic enzymes for the endocannabinoids are found intracellularly, are typically associated with the putative transporter, and are probably delivered endocannabinoids by a protein carrier[53]. Fatty acid amide hydrolase, expressed in two versions (FAAH and FAAH2)[54,55], is responsible for the breakdown of anandamide into arachadonic acid and ethanolamine. FAAH is found in particularly high concentrations in the hippocampus, cortex, and cerebellum[56], suggesting that anandamide is more tightly controlled in those regions. To a lesser extent, anandamide is also catabolized by *N*-acylethanolamine acid amidase (NAAA)[57]. 2-AG is broken down by monoacylglycerol lipase (MAGL)[58] and cyclooxygenase-2 (COX-2)[59]. In addition to the better known prostaglandins, COX-2 is also responsible for the creation of prostacannabinoids, which are themselves an active area of study[60].

Pathologies associated with CB_1 receptors

Due to the high density of CB_1 receptors in the brain, their distribution throughout the body, and the use of cannabis for its medicinal qualities since ancient times, it should not be surprising the CB_1 receptors have been implicated in several diseases. These diseases range from those in the central nervous system (CNS), to metabolic processes, to cancer[61]. The precise mechanism by which the endocannabinoid system and CB_1 receptors are involved in these diseases is complex and difficult to elucidate, as they could be either causing the pathologic process or responding to it in compensation of the primary cause. Nevertheless, several diseases are currently being investigated for their association with CB_1 receptors, which may provide new avenues for pharmacotherapy.

The psychoactive and mood altering nature of cannabinoid agonists was an early indication that CB_1 receptors may be involved in psychiatric disorders. The localization of CB_1 receptors in the limbic and cerebral cortex suggest that they may be involved in anxiety and mood disorders. Cannabis abusers have long observed the dose dependent, bidirectional effects that cannabis can have, producing euphoria and relaxation at small to moderate doses, and dyphoria and anxiety at higher doses[62]. Other factors, such as local environment and mood previous to cannabis administration can also affect this bidirectional phenomenon. These effects are likely due in part to CB_1 receptor mediated inhibition of GABA at lower concentrations, and glutamate at higher concentrations[63,64]. Pharmacological blockade and genetic deletion in rodents is thought to cause symptoms similar to depression[65], and indeed depression and suicidal thoughts was the cause for failure of CB_1 inverse agonists in humans (discussed below). In addition, a recent study has shown that polymorphisms in *CNR1* are associated with depression[16].

The role of CB_1 receptors in addiction has long been debated. As previously mentioned, mice lacking CB_1 receptors by genetic deletion do not demonstrate addiction to opioids[13]. Similarly, in models of alcohol dependence in rats, blocking CB_1 receptors has been shown to reduce intake of alcohol[66]. Similar findings have been found using other models of addiction[67], and are likely mediated by the endocannabinoid modulation of glutamatergic neurotransmission and dopamine release in the nucleus accumbens.

For many years case reports and anecdotal evidence existed for a correlation between cannabis use and schizophrenia. Often this correlation was bridged by the similarities of psychosis experienced by some cannabis abusers and schizophrenic patients[68]. A large study conducted in New Zealand uncovered a genetic susceptibility for those who experience psychosis after using cannabis to later develop schizophrenia[69]. A more recent study has shown a correlation between frequency of cannabis use with a lower age of diagnosis[70]. Other implications of the endocannabinoid system in schizophrenia include altered CB_1 receptor density in the corticolimbic region of schizophrenic patients, and sensitivity of neuregulin 1 protein to cannabinoids[71].

The particularly high density of CB_1 receptors in the basal ganglia as well as the classic cataleptic response from agonists has implicated CB_1 receptors in movement and neurological disorders. The neuromodulatory effects of the endocannabinoid system are responsible for striking a balance between excitation and inhibition, as can be illustrated in Parkinson's and Huntington's diseases, and in epilepsy. Parkinson's disease is defined by a decrease in voluntary movement due to insufficient dopamine signaling in the striatum, and is treated with dopamine replacement, which itself can cause dyskinesia. Early in the disease CB_1 receptor density is decreased, likely as a compensatory mechanism to rescue the decreased dopamine release. Late in the disease, endocannabinoid signaling is markedly increased, this time in compensation for overexcitation from other inputs in the brain[72]. Huntington's disease is marked by involuntary movements (chorea) and muscle spasms (dystonia), in addition to dementia, all of which emanate from degeneration in the cerebral cortex and basal ganglia. Decreased CB_1 receptor density and signaling has been well documented in

Huntington's disease[73], and likely contributes to the over excitatory signaling. In the case of epilepsy, an uncontrolled excitatory signal, such as from glutamate, can lead to an epileptic seizure. Thus it can be surmised the insufficient endocannabinoid activity could contribute to this uncontrolled release of glutamate, which indeed appears to be the case[74,75].

The hyperphagia associated with cannabinoids has been documented since ancient times, and thus the endocannabinoid system has become a target for metabolic disorders in modern times. The initial rationale for developing a CB_1 receptor antagonist or inverse agonist was to simply block or reverse the natural appetite stimulating property of CB_1 receptor activation, thereby reducing weight. After further development of pharmacotherapy, it was discovered that inverse agonists for the CB_1 receptor also improved symptoms and biomarkers for metabolic syndrome in addition to decreasing appetite. Studies in rodents have further established that acute weight loss occurs by CB_1 receptors blocked in the brain and reduced food intake, but after approximately one week continued weight loss was achieved by receptors blocked in the periphery and increased metabolism[76,77]. Other studies have suggested that CB_1 receptors are dysregulated in some genetic causes of obesity[78], or after a continuous high fat diet[79].

Development of pharmacotherapy

Humans have sought to master the therapeutic benefits possible through cannabinoid receptors for thousands of years. Cannabis has been smoked and consumed in its raw form for at least 3,000 years, was long used as an appetite stimulant, analgesic, anti-inflammatory, and decongestant, and was used to treat conditions ranging from headaches to malaria[80]. By the nineteenth century many pharmacists attempted to isolate and purify the active ingredients of cannabis, since the dosing and effects of the drug were highly variable in its raw form. However, unlike other drugs successfully extracted from plants such as quinine, morphine, and cocaine, cannabis extract is very sticky and lipophilic, making it difficult to isolate and crystallize individual components. By the early twentieth cannabis extracts that contained inconsistent amounts of cannabinoids were available as syrups, tinctures, and pills[81], however pharmaceutical development then slowed when marijuana was designated a controlled substance and more reliable medicines became available.

Improved chemical methods of chromatography and spectroscopy permitted the isolation and identification of the active components of cannabis. The modern age of cannabinoid pharmacology began in 1964 when Gaoni and Mechoulam identified Δ^9-THC as the pharmacologically relevant compound in cannabis[25]. Around the same time cannabinoids with various potencies and receptor selectivity, such as cannabinol and cannabidiol, were also discovered. This led to a resurgence of interest in using cannabinoids for clinical remedies. Dronabinol (Δ^9-THC) is currently indicated for appetite stimulation in AIDS, and for nausea and vomiting associated with cancer chemotherapy. Sativex®, a spray containing Δ^9-THC and cannabidiol in nearly equal amounts, has been approved for use in multiple sclerosis and as an adjunct analgesic for cancer associated pain. Additional indications for cannabinoids are currently under

research. Meanwhile, acceptance of smoked cannabis for medical purposes is growing in the United States, with 13 states currently permitting licensed use of the drug.

The development of highly selective inverse agonists for the CB_1 and CB_2 receptors provided a means to avoid the poor selectivity and psychotropic effects associated with agonists, and initiated a new mechanism of therapy. Rimonabant (Sanofi-Aventis), the first selective CB_1 receptor inverse agonist[40], was available in Europe for the treatment of obesity with metabolic comorbidity. Several clinical trials[82-86] demonstrated significant weight loss when patients were given rimonabant combined with a calorie-reduced diet, in addition to increased HDL, decreased triglyceride levels, decreased hemoglobin A1c, increased circulating adiponectin, and increased lipoprotein particle size, all of which are improvements of comorbid biomarkers for obesity and insulin resistance. Additional trials investigating rimonabant for use in alcohol dependence[87] or smoking cessation[88] have showed favorable effects, however the results were either insignificant or inconclusive. Unfortunately, nearly all of these trials reported significant adverse effects including depression, anxiety, and intolerable gastrointestinal effects. The psychiatric side effects were of concern to the Food and Drug Administration (FDA), and were the reason why rimonabant was not approved for use in the United States until additional data was collected[89]. After additional data in Europe was collected regarding the efficacy and side effects of rimonabant in clinical practice, the risk to benefit profile of the drug became unfavorable. Subsequently, the European Union suspended rimonabant from the market. Another inverse agonist for the CB_1 receptor in clinical trials, taranabant (Merck), demonstrated a dose dependent response to the same adverse effects. Taranabant is structurally different from rimonabant, suggesting that these side effects were mechanism dependent and not specific to rimonabant. In response, Merck and several other pharmaceutical companies withdrew their compounds from clinical development[90].

These events may appear to be a setback for cannabinoid pharmacology, however several new approaches are under development. While the initial rationale for CB_1 receptor blockade was to decrease appetite in the brain, inverse agonists had favorable effects on metabolic processes which were likely mediated by peripheral CB_1 receptors[91]. Thus, an inverse agonist for the CB_1 receptor that is peripherally restricted, such as JD-2114 or JD-5006, should mediate the favorable metabolic effects, while avoiding the intolerable psychiatric effects[92]. Other approaches to CB_1 pharmacotherapy, such as the inhibition of endocannabinoid metabolism, are currently under development and may provide another avenue for treatment in anxiety and depression. Currently, URB597, a FAAH inhibitor, is being investigated in clinical trials, and has shown promise in rodents and monkeys[93]. It is interesting to note that we may have been unwittingly using pharmacotherapy targeting the endocannabinoid system for over 50 years. Acetominophen (paracetamol), a widely used pain reliever which has long lacked an understood mechanism, is metabolized *in vivo* into AM404, an inhibitor of the putative endocannabinoid transporter known to reduce pain[94,95].

Our understanding of the endocannabinoid system, its role in disease, and its availability for pharmacotherapy will continue to grow. Due to the complexity of the endocannabinoid system, improved methods for directly probing and monitoring it *in*

vivo are needed for future research. Thus, imaging the CB_1 receptor *in vivo* will be a tremendous advance as we attempt to further our understanding of the endocannabinoid system.

POSITRON EMISSION TOMOGRAPHY

Positron emission tomography (PET) is an imaging technique that capitalizes on the unique properties of positron emitting isotopes[96]. These unstable isotopes contain fewer neutrons than the more common stable isotope (*e.g,*. ^{11}C *vs.* ^{12}C), and attain stability by emitting a positron from a proton in the nucleus (Fig. 4). The parent proton then transmutes into a neutron, and the ejected positron travels a short distance before encountering an electron. The positron, which has the same mass but opposite charge of the electron, annihilates with the electron in a momentum conserved collision. As a result, their mass is converted into energy in the form of identical gamma rays 180^o apart with energy of 511 keV each. Taking advantage of this geometry, PET incorporates radioactivity detectors, called scintillators, in a ring and records the time it takes each gamma ray to reach either side. Thus, by near-coincidence detection a three dimensional image can be constructed.

Many positron emitting isotopes are biologically important atoms, such as carbon, fluorine, nitrogen, and oxygen. Therefore, these isotopes can be incorporated into biologically active molecules and used to study living systems. Advantages of PET compared to other imaging techniques include the ability to image proteins and metabolic processes, and to do so with a high sensitivity (*i.e.*, can measure very low concentrations) and selectivity (*i.e.*, can select target of choice). Therefore, PET is a useful tool for imaging and quantifying neuroreceptors[97], and for psychopharmaceutical development[98,99]. The relatively short radioactive half-life of the isotopes minimizes the radiation dose to the subject; however it can also create challenges in synthesizing complex molecules in a short amount of time.

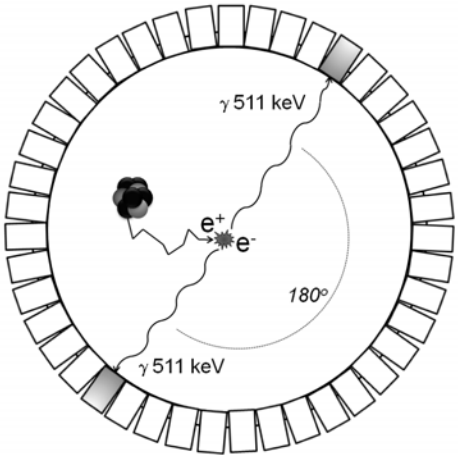

Figure 4. Physics of the PET camera. Positrons (e^+) are emitted from a proton within the nucleus of an isotope (*e.g.* ^{11}C, ^{18}F). The positron encounters an electron (e^-) and they annihilate, sending bidirectional gamma emissions of equal energy, which are coincidentally detected by the PET camera.

Principles in radiotracer design

A major challenge in PET research is the design and evaluation of successful radioligands. Successful radioligands used in PET studies differ in quality from those used for *in vitro* studies[100], or from compounds typically considered for pharmacotherapy[101]. Unlike *in vitro* studies in which radioligand can be washed away,

radioligands used *in vivo* should dissociate from their target and wash out of the tissue within a reasonable period of time so that pharmacokinetic measurements can be made. Likewise, compounds considered for drug development may not always be candidates for use in PET due to high non-specific binding, high plasma protein binding, or metabolite profile. Drugs developed for clinical therapy often have a large area under the curve (*i.e.*, available in concentrations that have therapeutic effect for a long time), which would be associated with pharmacokinetics too slow for a reversibly binding PET tracer. In addition, drugs for clinical therapy do not require as high a selectivity or specific binding as a PET tracer does.

An ideal radioligand for use in PET should have several properties (Table 1)[98,102-4]. Due to the short half-life of PET radioisotopes, radiolabeling of a PET tracer must be done quickly and easily. The radioligand should have a high concentration of radioactivity (specific activity) to avoid significant receptor occupancy and pharmacological effects, and be prepared in a safe formulation. Once injected, a radioligand must easily enter the brain with high uptake, and not be a substrate for any efflux transporters. Once in the brain, the radioligand should bind only to the receptor of interest (high selectivity) with sufficient binding affinity, and have a high signal to noise ratio (low non-specific binding). In order to facilitate pharmacokinetic modeling, the radioligand should bind reversibly from the receptor, allowing it to washout of brain within the scan time, and potentially be displaced by another ligand, whether agonist, antagonist, or inverse agonist. In the periphery, the radioligand should be cleared quickly, and not be metabolized into radioactive metabolites that can cross back into the brain.

Table 1. Characteristics of successful PET radioligands

"Typical" radioligands	**CB_1 receptor radioligands**
Low lipophilicity	*Moderate lipophilicity*
Penetration and high uptake in brain	
High affinity	Moderate to high affinity
Reversible binding and washout within scan time	
High selectivity	
Low non-specific binding	
No accumulation of radiometabolites in brain	
Easily radiolabeled with PET isotope	
Lack of efflux transporter affinity	
High specific activity	Moderate specific activity acceptable

Radioligands for the CB_1 receptor should follow the guidelines outlined above, with a few possible exceptions. First, cannabinoid ligands are quite lipophilic (due to the transmembrane domain binding site) and are prone to binding non-specifically to lipids and proteins in brain, or binding avidly to proteins in plasma, preventing their entry into brain. Therefore, radioligands for the CB_1 receptor should have a moderate lipophilicity, which may be higher than more typical PET radioligands. Second, Δ^9-THC and several other cannabinoid ligands are partial substrates for the P-glycoprotein efflux transporter[105], and thus careful screening of potential candidate ligands should be executed to ensure they are not substrates as well. Third, the receptor density of CB_1 receptors in brain is very high, and thus the binding affinity need not be as high as that for other receptors found with much lower densities. Finally, due to the high density of

CB_1 receptors, the requirement for high specific activity needed for most radioligands would not be expected to be as strict.

Pharmacokinetic modeling

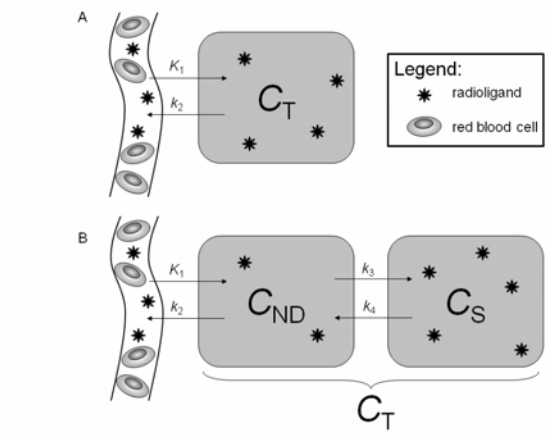

Figure 5. Tissue compartment models. A) The one-tissue and B) two-tissue compartment models depict the kinetics (K_1, k_2, k_3, k_4) and concentration of radioligand in blood and tissue (C_T). The two-tissue compartment model accounts for radioligand that is non-displaceable (C_{ND}) and specifically bound (C_S).

A major advantage of PET imaging is the ability to quantitatively measure radioactivity in a target organ. In the case of neuroreceptor imaging, this means that receptor density can be quantified if an appropriate PET ligand is used correctly. The quantitative method will vary depending on the characteristics of the receptor and the radioligand, both of which influence the pharmacokinetic model used during analysis. The purpose of the pharmacokinetic model is to describe the observed data in a physiologically meaningful way, quantitatively, and accurately. A complete derivation and discussion of pharmacokinetic models used in PET may be found elsewhere[106] a condensed description relevant to this thesis is provided below.

The standard pharmacokinetic models for neuroreceptor imaging are the one- and two-tissue compartment models. In brief, these assume that radioligand delivered by arterial blood will be taken up into a tissue until equilibrium is reach between the freely available radioligand in the blood and tissue (Fig. 5A). In the one-tissue compartment model, the concentration of radioligand would be dependent on the rate of entry, the rate of exit, and the concentration of radioligand in the blood and tissue:

$$\frac{dC_T(t)}{dt} = K_1 C_P(t) - k_2 C_T(t) \qquad \text{(Eq. 1)}$$

The rates of entry (K_1) and exit (k_2) are defined by rate constants. The concentration of radioligand observed in the tissue compartment (C_T) would be dependent upon the concentration of radioligand available in the plasma, which varies over time as radioligand in plasma is cleared. The concentration of radioligand in plasma (C_P) over time can be measured and modeled independently, and is termed the input function. Mathematically, these can be recombined and described as a convolution:

$$C_T(t) = K_1 e^{-k_2 t} \otimes C_P \qquad \text{(Eq. 2)}$$

Following a bolus injection, the convolution can be solved with an impulse response function and subsequently integrated, which reduces to:

$$\int_0^\infty \frac{C_T(t)}{dt} = K_1 \int_0^\infty e^{-k_2 t} \bullet \int_0^\infty \frac{C_P(t)}{dt} \quad \text{(Eq. 3)}$$

$$C_T = \frac{K_1}{k_2} \bullet C_P \quad \text{(Eq. 4)}$$

where C_T and C_P are the respective concentrations in tissue and plasma integrated from time of injection to infinity. The ratio of the two is called distribution volume (V_T):

$$V_T = \frac{C_T}{C_P} = \frac{K_1}{k_2} \quad \text{(Eq. 5)}$$

Note that this is equivalent to the relationship of the two compartments and their rate constants during steady-state equilibrium. That is, when the two compartments reach equilibrium:

$$C_P \bullet K_1 = C_T \bullet k_2 \quad \text{(Eq. 6)}$$

In the two-tissue compartment model, the radioligand can be conceptualized as being in a "non-displaceable compartment," which represents radioligand non-specifically bound to proteins or lipids or is free in tissue, and a "specifically bound" compartment, which represents radioligand bound to a receptor (Fig. 5B). Similar to Eq. 1, the two compartments can be described as:

$$\frac{dC_{ND}(t)}{dt} = K_1 C_P(t) - k_2 C_{ND}(t) - k_3 C_{ND}(t) + k_4 C_S(t) \quad \text{(Eq. 7)}$$

$$\frac{dC_S(t)}{dt} = k_3 C_{ND}(t) - k_4 C_S(t) \quad \text{(Eq. 8)}$$

As in the one-compartment model, the rate of radioligand entering and exiting the second compartment is determined by rate constants, k_3 and k_4. Both compartments are observed in tissue together by the PET camera. Thus,

$$C_T = C_{ND} + C_S \quad \text{(Eq. 9)}$$

After combining Eqs. 7 and 8 into Eq. 9, the full derivation of distribution volume reduces to:

$$V_T = \frac{C_T}{C_P} = \frac{K_1}{k_2} + \frac{K_1 k_2}{k_3 k_4} \quad \text{(Eq. 10)}$$

Based on these models (Fig. 5) and the derivations above, one can attribute the physiological relevance of the parameters in Eq. 10 to *in vivo* imaging with respect to a radioligand[107]:

K_1 is the rate constant of entry from arterial plasma into brain tissue

k_2 is the rate constant of exit from brain back to arterial plasma

k_3 is the rate constant of binding to the receptor, which is determined by the amount of radioligand free in the non-displaceable compartment, the number of receptors available for binding, and the rate of association (*i.e.*, binding) to the receptor

k_4 is to the rate constant of dissociation from the receptor

V_T is distribution volume, and at equilibrium is proportional to receptor density

Mathematically, one can see how distribution volume can be described in two ways: by integrals and by rate constants. The ratio of integrals, or areas under the curve, of radioligand in tissue (*e.g.*, brain) divided by radioligand in arterial plasma gives a conceptual understanding to the definition of distribution volume. Over the course of the entire study the brain was exposed to the amount of radioligand available in plasma (*i.e.*, the input function), and the brain responded by taking up the radioligand (Fig. 6). Unfortunately, we cannot always measure the complete area under the curve because of the short radioactive half-life or slow pharmacokinetics of the radioligand. Fortunately, distribution volume can also be described using rate constants (Eqs. 5 and 10). If the input function is known, then an iterative computational estimate of the rate constants can be performed that best matches the tissue curve. An iterative process is necessary because it is impossible to perform a reverse convolution. This analysis can be performed with only part of the entire curve of brain or plasma data, however enough of the curve-shape must be observed for it to be successful, in particular the tissue uptake, peak, and initial decline.

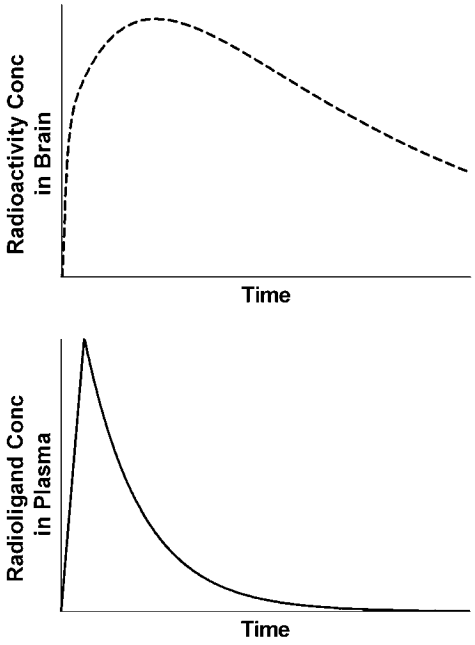

Figure 6. Example of time-activity curves. Distribution volume (V_T) is equal to the AUC of radioactivity in brain divided by the radioligand in plasma taken to an infinite time.

A few assumptions need to be observed when considering the pharmacokinetic models described here. It is important to keep in mind that what is measured during a PET study is radioactivity in brain and radioligand in plasma. Therefore, radioactivity not

due to parent radioligand (*e.g.*, radiometabolites) that enter brain cannot be distinguished from radioactivity in brain due to the parent radioligand, and could cause an overestimation of V_T. Second, PET uses tracer concentrations of radioligand, which assumes the radioligand is given in amount too small to have a pharmacological effect, yet represents the entire population of targets. Finally, these PET experiments assume the system being probed is unchanging during the study (*e.g.*, the number of receptors available are constant).

Considerations in translational research with PET

Translational research can be defined as "studies at the interface of the bench and bedside" for which "the information flow is bidirectional[108]." Currently, the development of PET radioligands for human use is primarily conducted by this method, where a candidate radioligand is discovered in the laboratory, evaluated in animals, tested in humans, and possibly refined in the lab and/or animals before being tested again in humans. Generally, new radiolabeled compounds are tested in rodents or non-human primates to investigate their brain penetration, degree of specific binding, and to ensure the lack of pharmacological effects. This discovery process is highly favored due to its decreased development time and cost compared to traditional drug discovery[109]. However, these model species are not always predictive of how PET radioligands may behave in humans, as there may be dramatic interspecies differences in drug disposition and targeting. In addition, appropriate preparations should be made before commencing a PET study in humans.

An example of the dramatic differences in drug metabolism between species can be illustrated with the PET radioligand [^{18}F]SP203. Initial studies of [^{18}F]SP203 in rodents demonstrated that it was metabolized in the brain by a glutathione transferase mechanism, trapping radiometabolites in the brain[110]. Subsequent studies in monkeys showed that it was quickly metabolized in blood, creating radiometabolites that could enter the brain. However, human studies with [^{18}F]SP203 have not reproduced either of these metabolic processes, and [^{18}F]SP203 has been demonstrated to be a useful PET tracer for mGluR5 receptors in human[111]. If preclinical studies had decided the fate of [^{18}F]SP203, it would probably not have been considered a hopeful candidate compound, and its success in human would not have been realized.

A common problem in PET radioligand development is the susceptibility of candidate compounds to be effluxed from the brain by the permeability-glycoprotein transporter (P-gp), the gene product of *MDR1*[112]. For this reason, new radioligands are often tested in wild type and P-gp knockout mice or in monkeys before and after treatment with P-gp inhibitors. However, the interspecies difference of P-gp selectivity can be dramatic, as reflected by the relatively low amino acid sequence homology[113].

In addition to differences in metabolism and brain penetration of potential PET radioligands, the characteristics of the intended target may be different between species. For example, several radioligands have been developed for imaging translocator protein (18kDa) (formerly known as peripheral benzodiazepine receptor, PBR), a biomarker for inflammation. In non-human primates, these compounds generally show

appreciable brain uptake and are quantified by two-tissue compartment models. When studied in humans, these PET tracers show much less brain uptake, and modeling can be confounded by a large amount of non-specific binding. The explanation lies partially in the fact that TSPO is expressed approximately 20 times more in non-human primate brain than in human brain[114].

With so many potential pitfalls in extrapolating data from animals to humans, when is it appropriate to use animals for PET radioligand development? Animals should be used when a procedure would otherwise cause death, disability, or undue pain in a human. For example, disease models involving neurotoxic drugs or certain stress-inducing psychiatric experiments would be unethical in humans. However, animals must be tested and euthanized in a humane manner, and their use should be reduced, refined, and replaced whenever possible. Second, animals should be used when a procedure has unknown consequences in a human. This would be the case for any new drug; PET radioligands are typically administered at tracer doses, which by definition are below pharmacologically active concentrations. Nevertheless, caution would dictate that new radioligands be briefly tested in animals before injected into humans. Finally, animals should be used when it would be otherwise impossible to obtain information from human, *in vitro*, or *in silico* experiments. For example, mice with inactivated genes (knockout mice) can provide information on gene expression, function, and pathophysiology that is impossible in humans[115]. While certain *in vitro* and *in silico* assays are under development for predicting a PET tracer's P-gp affinity[116] or brain uptake and non-specific binding[117], such models need to be verified by *in vivo* findings, and therefore animals are still preferred.

PET reduces the overall burden of research in both animals and humans, providing *in vivo* information on pharmacokinetics, pharmacodynamics, and neurochemistry by non-invasive means. For example, PET studies can provide evidence for future efficacy of novel therapeutics[118] thereby shortening drug development time, and facilitate diagnosis of diseases confirmed only by autopsy[119]. Accelerating drug development and improving diagnostic procedures would impact populations of patients, and so PET studies conducted for that purpose must be properly designed and powered. Compared to other research modalities such as genetics or MRI, studies with PET typically use smaller sample sizes due to cost and availability. However, large variability of the measured parameter(s) may exist within a healthy or patient population, which may increase the chance of type I or II error in a study. Thus, careful consideration must be given to the study methods and design in order to maintain the benefits of knowledge gained over the risks exposed to research subjects.

The quantitative methods for accurately analyzing data from PET studies in brain can become quite rigorous and can demand measurements that are considered invasive. By itself PET imaging is considered a non-invasive procedure, and much qualitative and quantitative information can be garnered from the resulting images alone. However when developing and evaluating a new radioligand for PET, assurances must be made that the radioactivity observed either represents or can be corrected to represent the actual concentration of the desired target (*e.g.*, receptor, transporter, enzyme, etc.). This can be achieved in multiple ways; however none of them are without risk. The most

accurate, and most invasive, method would be to simultaneously measure radioactivity in brain while directly measuring the chemical composition and target density in brain. A much less invasive method involves the use of an arterial catheter in the wrist to measure the concentration of parent radioligand in arterial plasma over time, which is used as an input function (described previously in "Pharmacokinetic modeling"). This technique cannot directly measure whether confounding radiometabolites enter the brain, and the placement of an arterial catheter can be painful and, rarely, can result in lasting pain or numbness. Probably the least invasive technique for analyzing PET data quantitatively is by comparing a target rich brain region with a target devoid brain region, otherwise known as a reference region. Typically, a reference region has been verified to have no specific binding by the radioligand in either post-mortem brain samples or *in vivo* after pharmacological doses of an antagonist. In some cases there may not be a suitable reference region available for a particular target, and this method would not provide accurate results if used to measure target density. Error or false assumptions in any of these qualitative methods increase the chance that results do not represent true findings, and decrease the risk to benefit ratio.

A limitation of PET studies in human is the use of radioactivity. The impact and effect of radiation exposure from a typical PET study on human health are not completely agreed upon[120]. Therefore, research using PET should be well designed to ensure that the general benefit of knowledge gained outweighs the risk involved with radiation exposure. Such preparations include the estimation of radiation dose anticipated from the study (summarized as effective dose), the proper amount of injected radioactivity for the study, and determining the minimum time required to complete the study before substantial radioactive decay. In clinical research, the burden of radiation exposure falls on the subjects enrolled in the study. A good radioligand with high selectivity, specificity, and good pharmacokinetics will provide superior accuracy and precision, requiring fewer subjects to reach the study endpoints, reducing the overall radiation burden.

PET IMAGING OF CB_1 RECEPTORS

Due to the involvement of cannabinoid receptors in numerous diseases and their potential for targeted drug development, the desire for a radioligand to image cannabinoid receptors quickly emerged. Before a radioligand that directly targets the CB_1 receptor was developed, PET studies attempting to unlock the effects of cannabinoids were performed using [^{15}O]water or [^{18}F]FDG[121-123]. While these studies are interesting, their measure of blood flow and metabolism in the brain do not directly probe CB_1 receptors. Recent advances in CB_1 pharmacology have improved the selectivity of candidate radioligands, and decreased lipophilicity has improved their uptake in brain, allowing direct imaging of the CB_1 receptor.

Early attempts

The development of a selective radioligand for imaging the CB_1 receptor has been an area of intense interest and struggle for many years. The first attempt at designing a radioligand for CB_1 receptor imaging took the logical approach of radiolabeling a close

analogue of Δ^9-THC[124]. Unfortunately, the relatively low affinity and high lipophilicity of ((-)-5'-[^{18}F]Fluoro-Δ^8-THC likely caused high non-specific binding and low availability of free radioligand in plasma (*i.e.*, that not bound to plasma proteins) able to cross into the brain. The discovery of rimonabant facilitated higher chemical selectivity for the CB_1 receptor, and as a result spawned the development of several CB_1 receptor-selective radioligands. [^{123}I]AM251 demonstrated increased selectivity for CB_1 receptors, however the high lipophilicity was again the likely cause of minimal brain uptake of the radioligand[125]. A closely related analog, [^{123}I]AM281/[^{124}I]AM281, had less lipophilicity, but also much less affinity for CB_1 receptors; as a result studies in patients with Tourette syndrome ([^{123}I]AM281)[126] and schizophrenia ([^{124}I]AM281) [127] demonstrated moderate uptake in brain and high non-specific binding. Two other radioligands, [^{18}F]AM5144 and [^{11}C]SR149080 (also known as [^{11}C]NIDA41020), were evaluated in monkey and were not considered for human use because of either high lipophilicity and poor brain uptake[128], or an insufficient signal expected in human brain[129].

"Second generation" ligands

Recently several promising PET radioligands for the CB_1 receptor have been reported with significant improvements over their predecessors. In the fall of 2006 the group from Johns Hopkins reported [^{11}C]JHU75528 in non-human primate brain[130]. Also known as [^{11}C]OMAR, the rimonabant-like compound was designed with a lower lipophilicity than its predecessors, while retaining high CB_1 receptor affinity. While [^{11}C]JHU75528 demonstrated moderate uptake in mouse and baboon brain, the analytical method for quantitation of CB_1 receptors used a reference tissue model based on either thalamus or pons as a background region. Though the results of this method correlated with results using compartment modeling, the validity of this model would be contingent on thalamus and pons being devoid of CB_1 receptors; autoradiography[22] and other PET studies (Burns et al., 2007 and Yasuno et al., 2008; discussed below) indicate they are not. In addition, in spite of the relatively fast kinetics of the radioligand, quantitative measurements of [^{11}C]JHU75528 in brain did not reach stable measurements in mice or baboons within the observation period. Additional work using [^{11}C]JHU75528 in humans has been reported, but the detailed results, such as kinetic modeling data and parameter variability, have not yet been released[131,132]. Analogs of [^{11}C]JHU75528 recently designed with decreased lipophilicity and CB_1 receptor binding affinity have been evaluated in mice, which suggests they may be improved radioligands for *in vivo* imaging[133].

In the spring of 2007 the group from Merck Research Laboratories reported [^{18}F]MK-9470 in humans and non-human primates. An analog of taranabant, [^{18}F]MK-9470 has a 60-fold selectivity for CB_1 over CB_2 receptors, is not a P-gp substrate *in vitro*, has moderate lipophilicity, and good entry into brain[134]. In both monkeys and humans, radioactivity increased in brain up to about 120 minutes after bolus injection with [^{18}F]MK-9470, and concentrations of radioactivity did not appear to decline, even though concentrations of the radioligand in arterial plasma decreased throughout the length of the scan[135]. For these reasons, brain studies using [^{18}F]MK-9470 were analyzed using a pharmacokinetic method designed for irreversible PET radioligands[136]

which simply uses the area under the curve (AUC) of radioactivity in brain after a period when measurements have stabilized (*e.g.*, 120 – 180 minutes after injection). However, when challenged with taranabant the radioactivity quickly washed out of brain, indicating that [^{18}F]MK-9470 undergoes reversible binding at the CB_1 receptor. Nevertheless, using this analytical method the authors found [^{18}F]MK-9470 had good precision (retest variability <7%) and intersubject variability (16%), and could be utilized in receptor occupancy studies with taranabant[135,137]. Several other studies using [^{18}F]MK-9470 have since been reported, such as an investigation of brain uptake in rats after treatment with antiepileptic drugs[138], a demonstration of increased CB_1 receptor availability with age in women but not in men[139], and an association of decreased CB_1 receptor availability in healthy subjects with novelty-seeking temperament[140]. While the results of these studies are intriguing, they were analyzed without correcting the amount of radioactivity in brain by the amount of radioligand in arterial plasma, and are therefore susceptible to pharmacokinetic variables from the periphery that may affect the delivery of the radioligand to brain (*e.g.*, metabolism, distribution, excretion which could change radioligand concentration).

Imaging [^{11}C]MePPEP in monkey brain

A third PET radioligand for CB_1 receptors, [^{11}C]MePPEP, was created in a collaborative effort between Lilly Research Laboratories, the National Institute of Mental Health, and Karolinska Institutet. [^{11}C]MePPEP was designed to have high affinity and selectivity for the CB_1 receptor, yet have a more moderate lipophilicity compared to earlier attempts at CB_1 receptor PET tracers. Compared to rimonabant MePPEP has about 10 times higher binding affinity, and has >700 times greater selectivity for CB_1 than CB_2.

The first publication of [^{11}C]MePPEP reported results in rhesus monkey[141], and was released at about the same time as [^{11}C]JHU75528 and [^{18}F]MK-9470. Like [^{11}C]JHU75528 and [^{18}F]MK-9470, [^{11}C]MePPEP demonstrated reversible binding with high specificity and selectivity for the CB_1 receptor; however [^{11}C]MePPEP had higher uptake in brain (almost 600% SUV) than either of the other two radioligands. Serial measurements of radioactivity in brain and parent radioligand in arterial plasma were used to estimate distribution volume. When assessed by compartmental analysis and pharmacological blockade, the specific binding of [^{11}C]MePPEP was approximately 89%. Similar to results found with [^{18}F]MK-9470, there did not seem to be any region of the brain that was completely devoid of specific binding; even the pons, a region of low CB_1 receptor density, demonstrated 70% specific binding. After inhibiting P-gp transporters with the drug DCPQ, brain uptake increased by about 17%. However, since free fraction also increased by 10% it was concluded that the increased brain uptake was due to displacement of radioligand from plasma proteins by the P-gp inhibitor, and that [^{11}C]MePPEP is not a significant substrate for P-gp.

The authors also pointed out some limitations of [^{11}C]MePPEP that could be problematic in future studies. First, the free fraction of [^{11}C]MePPEP, the fraction that was not bound to proteins in arterial plasma, was very low, about 0.05%. Such a low free fraction may have prohibited radioligands for other targets from any appreciable

accumulation in brain, however the extremely high density of CB_1 receptors in brain was likely the reason this low free fraction was overcome. Nevertheless, a low free fraction remained a concern, since seemingly small changes in the bound fraction could have dramatic changes in free fraction. For example, a change of bound fraction from 99.9% to 99.8%, which could be caused by competitive binding by a drug, would correspond to a change of free fraction from 0.1% to 0.2%, or a 100% increase. Second, it was unknown if any radiometabolites generated from [^{11}C]MePPEP were present in brain. The authors pointed out that an assessment of radiometabolites in brain should be investigated if [^{11}C]MePPEP were to be used in humans. Finally, the relatively slow washout of [^{11}C]MePPEP from monkey brain raised concerns that if a slower washout rate were observed in humans, the radioactive half-life of ^{11}C would limit the time needed to attain accurate measurements of distribution volume.

The results obtained from rhesus monkey were promising that [^{11}C]MePPEP might be a clinically useful radioligand for PET imaging of CB_1 receptors. Further evaluation confirming the lack of P-gp affinity, the specificity for CB_1 receptors, and the ability to determine distribution volume parameters in a clinically relevant time with [^{11}C]MePPEP were warranted. Additionally, investigation was needed to assess if an endogenous agonist could displace [^{11}C]MePPEP, which would allow the radiotracer to be used assess endocannabinoid tone. Finally, estimates of radiation exposure resulting from clinical scans needed to be calculated in order to assess the radiation burden anticipated in future studies.

AIMS

1. To completely assess the *in vivo* properties of [^{11}C]MePPEP as a PET tracer in rodents (paper I).

2. To determine if [^{11}C]MePPEP is suitable to image and quantify CB_1 receptors in human brain. (paper II).

3. To determine if [^{18}F]FMPEP-d_2 can provide more precise and accurate outcome measures than its analogue [^{11}C]MePPEP. (paper III)

4. To observe the biodistribution and to estimate the radiation dose expected from participating in scans with either [^{11}C]MePPEP or [^{18}F]FMPEP-d_2. (paper IV)

MATERIALS AND METHODS

A brief summary of methods, results, and discussion of the research on CB_1 receptor radioligands are presented here. Full copies of the published or submitted publications follow.

SUBJECTS

Studies in rodents included male Sprague-Dawley rats, age-matched P-gp knockout (*mdr-1a/1b*(−/−)) and wild type mice (*mdr-1a/1b*(+/+)), and CB_1 knockout (*CNR1*(-/-)) and wild type mice (*CNR1*(+/+)). All rodents were anesthetized with 1.5% isoflurane in oxygen, and body temperatures were maintained between 36.5 and 37.0 °C with a heating pad or lamp.

Studies in male rhesus monkeys were conducted at least 90 minutes after immobilization with ketamine, and maintained with 1-2% isoflurane anesthesia. Head movement was restricted in a stereotactic frame. Heart rate, blood pressure, and respiration were monitored throughout the length of the scan. Body temperature was maintained with a forced air warming unit. All animal procedures were performed in accordance with the Guide for Care and Use of Laboratory Animals and approved by the National Institute of Mental Health Animal Care and Use Committee.

All human subjects were free of current medical and psychiatric illness based on history, physical examination, electrocardiogram, urinalysis including drug screening, and blood tests including complete blood count, serum chemistries, thyroid function test, and antibody screening for syphilis, HIV, and hepatitis B. The subjects' vital signs were recorded before radioligand injection and several intervals afterwards. Subjects repeated urinalysis and blood tests within 24 hours after the end of the PET scan. All studies performed in human were approved by the local Institutional Review Board and were conducted under either an Exploratory Investigational New Drug or regular Investigational New Drug application submitted to the FDA.

RADIOLIGANDS AND PHARMACOLOGICAL DRUGS

The synthesis and radiolabeling of all radioligands used in this thesis has been described in detail in the doctoral thesis of Sean Donohue[142]. [^{11}C]MePPEP was studied in rodents and humans, [^{11}C]FMePPEP, [^{18}F]FEPEP, and [^{18}F]FMPEP were studied in monkeys, and [^{18}F]FMPEP-d_2 was studied in monkeys and humans (Fig. 7). All radioligands were obtained in high radiochemical purity (> 99%). Radioligands were administered to rodents as a bolus injection through either the tail vein (mice) or penile vein (rats), followed by small saline flush.

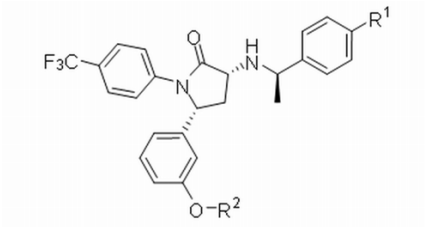

[^{11}C]MePPEP	R^1 = H, R^2 = [^{11}C]CH_3
[^{11}C]FMePPEP	R^1 = F, R^2 = [^{11}C]CH_3
[^{18}F]FEPEP	R^1 = H, R^2 = [^{18}F]CH_2CH_2F
[^{18}F]FMPEP	R^1 = H, R^2 = [^{18}F]CH_2F
[^{18}F]FMPEP-d_2	R^1 = H, R^2 = [^{18}F]CD_2F

Figure 7. Structure of [^{11}C]MePPEP and its analogues .

Radioligands were administered to rhesus monkeys and humans as a one minute infusion through either the tibial (monkey) or antecubital (human) vein, followed by a small saline flush.

All pharmacological challenges in rodents were administered at 40 min after radioligand injection, which was between 15 and 20 min after peak uptake of radioligand in brain. Rimonabant (3 mg/kg, IV) was administered in a dose known to displace [^{11}C]MePPEP in monkey brain[141]. Doses of CB_1 agonist agents anandamide, methanandamide, CP 55,940, and the FAAH inhibitor URB597 were chosen based on amounts reported to have central nervous system activity[93,143-145].

Radioligands assessed in rhesus monkeys were reassessed after pretreatment with rimonabant (3 mg/kg, IV), which was administered 30 minutes before radioligand injection. ^{11}C-radioligands were reassessed the same day, while ^{18}F-radioligands were reassessed three weeks after the initial assessment.

PET IMAGING

Studies in rodents were performed using the Advanced Technology Laboratory Animal Scanner (ATLAS)[146]. The ATLAS camera can accommodate a single rat or a pair of mice, allowing a paired wild type and knockout mouse to be imaged simultaneously. Serial dynamic scans began at the time of injection and continued with multiple frames of increasing duration from 20 seconds to 20 minutes, for 100 minutes over 23 frames. Images were reconstructed by a 3D ordered-subset expectation maximization algorithm into 17 coronal slices with 3 iterations, resulting in a resolution of about 1.6 mm full width at half maximum[147,148]. The data were not corrected for attenuation or scatter.

Studies with rhesus monkeys were performed in the high resolution research tomography (HRRT; Siemens/CPS, Knoxville, TN, USA), which has a reconstructed resolution of 2.5 mm at full-width half-maximum in all directions in 3D mode. A transmission scan was initially performed for attenuation correction. PET data was collected in multiple frames of increasing duration from 30 seconds to 5 minutes. Scans of 120 min (33 frames) were acquired in studies with ^{11}C-labeled radioligands, whereas longer scans (45 frames over 180 min) were acquired in studies with ^{18}F-labeled radioligands.

Human subjects participating in brain studies were scanned using a GE Advance camera (GE Healthcare; Waukesha, WI). Dynamic PET scans were acquired in 3D mode in multiple frames of increasing duration from 30 seconds to 5 minutes. Studies with [^{11}C]MePPEP lasted up to 150 or 210 min, and studies with [^{18}F]FMPEP-d_2 lasted up to 300 min. Subjects were given one 30 minute break during studies with [^{11}C]MePPEP lasting 210 min, and three 30 min breaks during studies with [^{18}F]FMPEP-d_2. Data were reconstructed with 3D filtered back-projection and a Hanning filter, resulting in an image resolution of 7.0 mm full width at half maximum. All PET images were corrected for attenuation and scatter. Head movement was restricted with a thermoplastic mask and was further corrected by intrasubject alignment during reconstruction. Subjects participating in the [^{11}C]MePPEP retest

studies had the test scan in the morning and the retest scan in the afternoon, whereas subjects participating in the [^{18}F]FMPEP-d_2 retest studies had at least 2 weeks between the test and retest scans.

Human subjects participating in the whole body studies were also scanned using a GE Advance, but with a different acquisition. In brief, each subject was imaged in seven contiguous 15-cm bed positions (head to upper thigh) in either 14 frames for [^{11}C]MePPEP or 16 frames for [^{18}F]FMPEP-d_2, each of increasing duration (15 seconds to 4 min) for a total scan time of 120 or 300 min, respectively. To minimize extraneous motion, head movement was restricted with a thermoplastic mask and subjects' arms and abdomen were wrapped with body-restraining sheets. All PET images were reconstructed with ordered subset expectation maximization image reconstruction and were corrected for attenuation. Subjects injected with [^{18}F]FMPEP-d_2 had three rest periods (30 min each) outside the camera, beginning at approximately 120, 180, and 240 min after injection. During this time, all voided urine was collected for measurement of radioactivity. The subject then returned to the scanner and was positioned in, and affixed to, the same approximate location on the bed as for the first scan. Five subjects studied with [^{18}F]FMPEP-d_2 collected their urine for 24 hours, from which radioactivity was measured the next day using a gamma counter that was cross-calibrated with the PET camera.

ANALYSIS

Tomographic images and kinetic data from all studies were analyzed with pixel-wise modeling computer software (PMOD Technologies, Zurich, Switzerland). Radioactivity was decay-corrected to time of injection and expressed as standardized uptake value (SUV), which normalizes for injected radioactivity and body weight:

$$\text{SUV} = \frac{\text{Radioactivity per g tissue}}{\text{Injected radioactivity}} \times \text{g body weight} \qquad \text{Eq. 11}$$

To estimate the density of CB_1 receptors in brain, an input function was analyzed as linear interpolation of the concentrations of radioligand in arterial plasma before the peak, and a tri-exponential fit of concentrations after the peak. Rate constants (K_1, k_2, k_3, and k_4) in standard one- and two-tissue compartment models[107] were calculated with weighted least squares and the Marquardt optimizer. Brain data of each frame of PET data were weighted by assuming that the standard deviation of the data is proportional to the inverse square root of noise equivalent counts. To correct the brain data for its vascular component, radioactivity in serial whole blood was measured and subtracted from the PET measurements, assuming that cerebral blood volume is 5% of total brain volume. The minimum scanning time necessary to obtain stable values of distribution volume (V_T) was determined by removing 10 minute segments of PET data from the terminal portion of the scan.

Regions of interest in rodent brain were identified relative to a rat[149] or mouse[150] brain stereotactic atlas. Genetic knockout mice were compared to wild-type mice, and pretreated rodents were compared to untreated rodents, by assessing the total area

under the curve (AUC) of radioactivity in brain. To estimate the density of CB_1 receptors in rat brain, blood was sampled under continuous flow from the femoral artery for the first 3 min, followed by intermittent samples until the end of the scan. Compartmental modeling in four rats using 2 h PET data and serial arterial plasma concentrations of [^{11}C]MePPEP separated from radiometabolites were used to compute distribution volume. To assess the presence of radioactive metabolites in rodent brain, brain tissues were harvested 30, 60, 90, and 120 minutes after radioligand injection.

Studies in monkeys were performed as previously described[141]. Arterial blood samples were collected from the femoral artery through an indwelling catheter. Monkeys receiving ^{11}C-radioligands were scanned and had blood sampled from 15 s to 120 min, while those receiving ^{18}F-radioligands were scanned and had blood sampled from 15 s to 180 min after radioligand injection. Specific binding was determined by:

$$\% \text{ Specific binding} = \frac{(V_T \text{ baseline} - V_T \text{ preblock})}{V_T \text{ baseline}} \times 100\% \qquad \text{Eq. 12}$$

For human brain studies, PET images were spatially normalized to a standard anatomic orientation (Montreal Neurological Institute, or MNI, space) based on transformation parameters from a magnetic resonance image (MRI). Normalizing PET images to the MNI template allowed use of a set of predefined volumes of interest from the automated anatomical labeling (AAL) atlas[151]. Six regions were defined from these preset volumes and analyzed: prefrontal cortex (303 cm^3), occipital cortex (172 cm^3), hippocampus including parahippocampus (32 cm^3), putamen (17 cm^3), thalamus (17 cm^3), and cerebellum (171 cm^3). Two additional regions, pons (6.5 cm^3) and white matter (8.3 cm^3), were not available from the AAL atlas, and thus were manually drawn on the MNI template and added to the AAL library of predefined volumes. To estimate the density of CB_1 receptors in human brain, blood samples were drawn from the radial artery from 15 seconds to 120 minutes for [^{11}C]MePPEP and 15 seconds to 270 minutes for [^{18}F]FMPEP-d_2. The plasma time-activity curve was corrected for the fraction of unchanged radioligand by radio-HPLC separation, as previously described[152].

In the whole body studies with [^{11}C]MePPEP, thyroid, brain, heart, lungs, liver, gallbladder, spleen, kidneys, red marrow, and intestine were visually identifiable as source organs. To estimate the residence time of red marrow and bone, regions of interest were placed on lumbar vertebrae and on radii and ulnae. To estimate the residence time of intestine, a large region of interest was placed on the abdomen. After injection of [^{18}F]FMPEP-d_2, brain, heart, lungs, liver, gallbladder, spleen, kidneys, bone, red marrow, intestine, and urinary bladder were visually identifiable as source organs. Lumbar vertebrae and radii and ulnae were again used to estimate the residence time of red marrow and bone. Large regions were placed to encompass all accumulated radioactivity in each organ.

CALCULATIONS AND SIMULATIONS

For all studies, group data are expressed as mean ± standard deviation (SD). Goodness-of-fit by the compartment models was determined with *F* statistics[153], the Akaike Information Criterion (AIC)[154] and the model selection criteria (MSC)[155]. The most appropriate model is that with the smallest AIC and the largest MSC values. The identifiability of the kinetic variables was calculated as the standard error (SE), which reflects the diagonal of the covariance matrix[156]. Identifiability was expressed as a percentage and equals the ratio of the SE to the rate constant itself. A lower percentage indicates better identifiability.

For studies in humans, intersubject variability was calculated as SD divided by the mean. Retest variability was calculated as the absolute difference between the test and retest studies, divided by the mean of the two. Intraclass correlation coefficient (ICC) was calculated for retest studies and compares the relative variation within subjects to between subjects. Values of ICC were calculated by:

$$\mathrm{ICC} = \frac{(\mathrm{BSMSS}-\mathrm{WSMSS})}{(\mathrm{BSMSS}+\mathrm{WSMSS})} \qquad \text{Eq. 13}$$

where BSMSS equals mean of summed squares between subjects, and WSMSS equals mean of summed squares within subjects. Values between 0 and 1 indicate that variability is higher between subjects than within subjects; values close to 1 suggest good reliability. Values between −1 and 0 indicate that variability is higher within subjects than between subjects and suggest poor reliability.

Simulations were performed as part of this thesis to aid in interpreting the relevance and impact of the results. The first simulation evaluated whether brain uptake of either [^{11}C]MePPEP or [^{18}F]FMPEP-d_2 is an accurate measurement of CB_1 receptor density in humans. The average input function and rate constants obtained from all human studies were used to calculate brain uptake and distribution volume (see equations from section on pharmacokinetic modeling). Increased and decreased receptor densities were predicted by corresponding changes in k_3. The expected number of subjects needed to detect these simulated changes in receptor density was estimated using the intersubject variability obtained from PET measurements. Estimation of sample sizes for a two-tailed independent samples *t*-test was made assuming α=0.05 (probability of type I error) and β=0.20 (probability of type II error, i.e., power of 80%). Another simulation analyzed the contribution of radioactivity from skull to that measured in brain based on resolution of the camera and the distance between skull and adjacent brain regions. Conservative assumptions were made that would tend to overestimate these values, and relative values of radioactivity measured in brain and skull were used to reflect collected data.

Radiation dosimetry estimates from human were calculated as follows. Organ uptake was corrected for radioactivity recovered (*i.e.*, the amount actually measured) by the PET camera. Some of the source organs were not confined to a single bed position and were calculated using a time point weighted by the average of organ radioactivity in the two frames. The area under the curve of each organ was calculated to the end of

imaging (120 min for [^{11}C]MePPEP, 300 min for [^{18}F]FMPEP-d_2) by the trapezoidal method. The area after the last image to infinity was calculated by assuming that further decline of radioactivity occurred only by physical decay without any biological clearance. The area under the curve of the fraction of measured injected activity from time zero to infinity is equivalent to the residence time. Residence time of bone was estimated based upon that in radius and ulna, which lack red marrow in adults[157], and extrapolated to that of all bone in the body. The residence time of all bone was divided between trabecular and cortical regions according to the mass ratio of these two regions (1:4). The residence time of red marrow was estimated from lumbar vertebrae after subtracting the bone component estimated from relative amounts in radii and ulnae. The residence time of all red marrow in the body was extrapolated from the 12.3% represented in lumbar vertebrae. The residence times for the intestinal tract were determined using the ICRP 30 intestine model[158], in which the highest percentage of injected activity measured in the intestines during the scanning session was designated as entering the small intestine. Total activity in the collected urine was added to that measured in the urinary bladder in the PET scan to determine total radioactivity excreted after injection. The cumulative activity in urine was decay corrected and expressed as a fraction of injected activity. The resulting curve was fitted with a mono-exponential function to estimate total radioactivity excreted at infinite time. To calculate the residence time of remainder of the body, the residence time of all source organs was summed and subtracted from the fixed theoretical value of $T_{1/2}$ / ln 2, which equals 0.490 hours for ^{11}C and 2.640 hours for ^{18}F. Radiation absorbed doses were calculated by the mean residence time for each source organ using OLINDA 1.0/EXM software[159] for a 70-kg adult male and a dynamic urinary bladder model, with voiding interval of 2.4 hours.

RESULTS AND DISCUSSION

PET IMAGING USING AN INVERSE AGONIST RADIOLIGAND TO ASSESS CANNABINOID CB_1 RECEPTORS IN RODENTS (PAPER I)

Rodents enabled us to evaluate [^{11}C]MePPEP in ways that would be either impossible, unethical, or expensive in either monkeys or humans. In addition, we were able to affirm that our results were not limited by a single experimental method.

We used genetically modified mice to confirm that [^{11}C]MePPEP is not a substrate for P-gp and has high specificity for the CB_1 receptor. First, when P-gp knockout mice were compared to wild type mice after injection of [^{11}C]MePPEP and scanned for 100 minutes, there was no difference between the two groups. This result was also found by *ex vivo* studies of wild type and P-gp knockout mice which corrected radioactivity in brain to radioligand in plasma. We also used CB_1 receptor knockout mice to find that approximately two-thirds of radioactivity after injection of [^{11}C]MePPEP is specific for CB_1 receptors in mouse brain (Figure 8A).

Rodents afforded us the chance to use high doses of drugs for pharmacological challenges against [^{11}C]MePPEP (Figure 8B). First, we found that rimonabant both blocked and displaced about two-thirds of the radioactivity in mouse and rat brain as assessed by PET, in agreement with our results using knockout mice. Second, we found that high doses of CB_1 receptor agonists were unable to cause any displacement or block of [^{11}C]MePPEP binding in brain. We used the endocannabinoid anandamide, a metabolically stable analogue methanadamide, the FAAH inhibitor URB597 (which raises anandamide concentration in brain) both alone and combined with anandamide, and the highly potent synthetic agonist CP 55,940 at doses that caused pharmacological effects. None of these challenges were able to cause any change in uptake or retention of [^{11}C]MePPEP in brain as assessed by PET. We confirmed these findings by *ex vivo* experiments using mass spectrometry, in which rimonabant caused >90% displacement of MePPEP, whereas CP 55,940 caused no displacement.

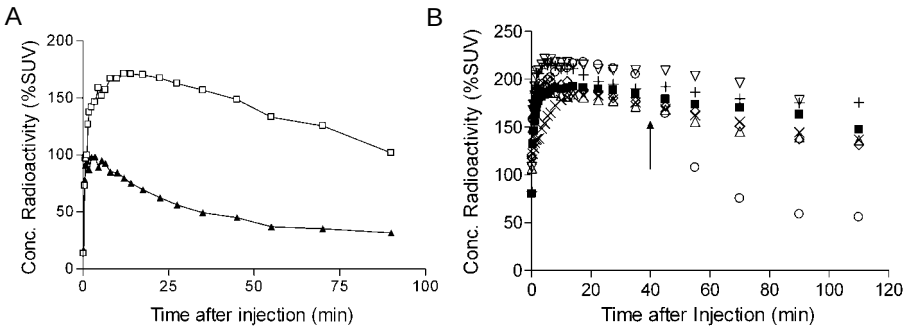

Figure 8. [^{11}C]MePPEP in rodent brain. A) Compared to a wild type mouse (□), the CB_1 receptor knockout (▲) mouse has about 1/3 radioactivity in brain. B) Drugs were administered IV to rats 40 min after [^{11}C]MePPEP. Compared to the baseline curve (■) inverse agonist rimonabant (○) displaced the majority of radioligand, whereas agonists anandamide (Δ), methanandamide (∇), CP 55,940 (◊), URB597 (anandamide reuptake inhibitor, ×), and URB597 with anandamide (+) were unable to displace the radioligandand.

Rodents also afforded us the ability to perform invasive procedures directly comparing [^{11}C]MePPEP in brain to observed radioactivity. Two such *ex vivo* studies have already been mentioned: those performed in P-gp knockout mice, and those performed in rats after pharmacological challenge with mass spectrometry. We also compared measurements of distribution volume over time to direct measurements of radioactivity composition in brain over time as assessed *ex vivo*. Using serial brain measurements and radioligand concentration from arterial blood, we found that distribution volume asymptotically reached a stable value over time, and that 90% of that value was reached within 70 minutes. While stable values of distribution volume generally assumes the absence of radiometabolites in brain, we found that radiometabolites of [^{11}C]MePPEP were present in brain, although at a constant percentage of about 13% from 30 to 120 minutes.

This study demonstrated that [^{11}C]MePPEP is not a substrate for the P-gp transporter, has high specificity for the CB_1 receptor, can be displaced by inverse agonists but not agonists, and that stable measurements of distribution volume can be attained within 70 minutes. Our studies confirmed the earlier findings in monkey that [^{11}C]MePPEP is not a P-gp substrate, and using P-gp knockout mice avoided confounding pharmacological effects of P-gp inhibitors which have previously been described[160] . The high specificity of [^{11}C]MePPEP for CB_1 receptors was observed in both knockout mice and receptor blockade in rats by PET (two-thirds specific), in addition to the *ex vivo* mass spectrometry analysis in rats (>90% specific). [The discrepancy was due in part to the constant percentage of radiometabolites in brain over time, which was not detected by the mass spectrometry method.] Thus, these results provide confirmatory evidence that [^{11}C]MePPEP is specific for CB_1 receptors, suggesting that similar results would be seen in human brain. The inability of [^{11}C]MePPEP to be displaced by agonist suggests a large receptor reserve; that is, a small percentage of CB_1 receptors are in the high affinity, agonist preferring, state. Such an observation is important when preparing for studies with [^{11}C]MePPEP in human brain, as it indicates that competitive agonist studies similar to those performed using [^{11}C]raclopride would not be possible. Finally, we have shown that stable measurements of distribution volume do not necessarily mean the absence of radiometabolites in brain. In addition, the presence of radiometabolites in brain should be considered during the analysis of [^{11}C]MePPEP and its analogues in human studies.

QUANTITATION OF CANNABINOID CB_1 RECEPTORS IN HEALTHY HUMAN BRAIN USING PET AND AN INVERSE AGONIST RADIOLIGAND (PAPER II)

While animal studies can suggest that a PET radioligand will be successful clinically, the true outcome is not evidenced until the first in human experience. Therefore, we sought to evaluate [^{11}C]MePPEP in humans and assess its ability to image and quantitate CB_1 receptors. We used the generally recognized "gold standard" method of compartmental modeling which incorporates serial measurements of radioactivity in brain and parent radioligand in arterial blood into the outcome measure of distribution volume (V_T), an index of receptor density.

Initial scans in human brain using [^{11}C]MePPEP demonstrated that radioactivity concentrated in areas with high CB_1 receptor density, and decreased slowly over the 150 minute study. The highest concentration of radioactivity in brain, typically achieved between 40 and 80 minutes after injection, had a relatively low intersubject variability (16%). When brain uptake of radioactivity was combined with concentrations of parent radioligand in arterial plasma to calculate V_T, we found that the intersubject variability for this composite variable was much higher (>60%).

Such discrepant intersubject variabilities would be expected if: 1) CB_1 receptor density was highly variable in our small sample; 2) our calculation of V_T was incorrect or unstable; or 3) our measurements of parent radioligand in arterial plasma were highly variable and had poor precision. The first supposition was unlikely based on studies with other PET radioligands, which typically have an intersubject variability of about 20-30%. This hypothesis would also be impossible to prove without directly measuring receptor density by invasive means. The second possibility was unlikely based on measurements of V_T over time, which indicated that V_T was consistently measured within about 60 minutes after injection of [^{11}C]MePPEP until the end of the 150 minute study. However, we did find that two subjects did not demonstrate stable measurements of V_T until 120 minutes after injection, which we thought might be due to the slow washout of radioactivity from brain. Therefore, we wanted to conduct additional studies that were longer than 150 minutes to ensure that we were obtaining sufficient data to calculate V_T accurately. Since the first two possibilities were unlikely, we suspected that the variability of V_T was primarily due to high variability and poor precision from our measurements of parent radioligand in arterial plasma. Indeed, we found that models of the plasma data reflecting the clearance of the radioligand resulted in values that were highly unstable or non-physiological. Unfortunately, we were limited by the low concentration of [^{11}C]MePPEP in plasma and the radioactive half-life of ^{11}C ($t_{1/2}$ = 20.4 minutes) such that we were not able to obtain meaningful measurements after 120 minutes.

We conducted a retest study with 210 minute scans to evaluate the precision of our measurements in brain and plasma (Fig. 9), and the precision and stability of V_T. We found that the plasma measurements were the cause for the high variability of V_T previously encountered. The retest variability (which is inversely related to precision) of plasma measurements was 58%, whereas the retest variability of brain uptake and V_T

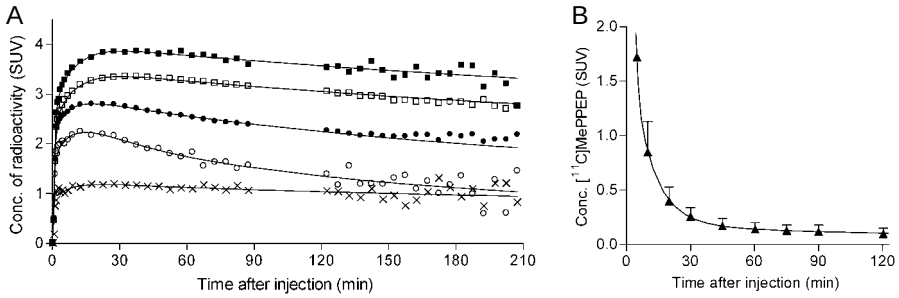

Figure 9. [^{11}C]MePPEP in human brain and plasma. A) Radioactivity in putamen (■), prefrontal cortex (□), cerebellum (●), pons (○), and white matter (×) were measured for 210 min, while B) radioligand (▲) could be measured in arterial plasma for only 120 min.

were 8% and 15%, respectively. Thus, the relatively poor precision of the plasma measurements contributed to the higher within and between subject variabilities of V_T compared to those of brain uptake. Nevertheless, our measurements of V_T were highly stable over time, and we obtained consistent values from 60 to 210 minutes after injection. In addition to demonstrating that V_T had good precision, the stability of V_T suggests the absence of any radiometabolite accumulation in brain. The ICC of V_T (*i.e.*, the sensitivity of distinguishing variability between subjects from within subjects) was considered good to excellent (0.87), and better than that that of brain uptake (0.77). Taken together, the stable measures of V_T, the high ICC of V_T, and the theoretically superior outcome measure of V_T compared to brain uptake suggests that V_T remains the more accurate index of CB_1 receptor density, in spite of the poor precision of plasma measurements.

We were curious as to how much impact the higher accuracy of V_T had, compared to the higher precision of brain uptake, on the sensitivity in detecting changes of CB_1 receptor density using [^{11}C]MePPEP. To this end we created a simulation that varied the receptor density by altering the quantitative model we derived from our subjects. We found that V_T was much more sensitive in measuring changes of receptor density, particularly when receptor density was increased (Fig. 10). By incorporating the intersubject variability acquired from our measured data, we estimated the number of subjects required to detect such changes in receptor density. We found the superior precision of brain uptake enhanced its sensitivity to detect changes in receptor density, since it required fewer subjects than V_T to predict a 50% decrease in receptor density (8 *vs.* 26 subjects, respectively). However, the high precision of brain uptake could not compensate for the superior accuracy of V_T in predicting a 50% increase of receptor density (25 *vs.* 26 subjects required, respectively).

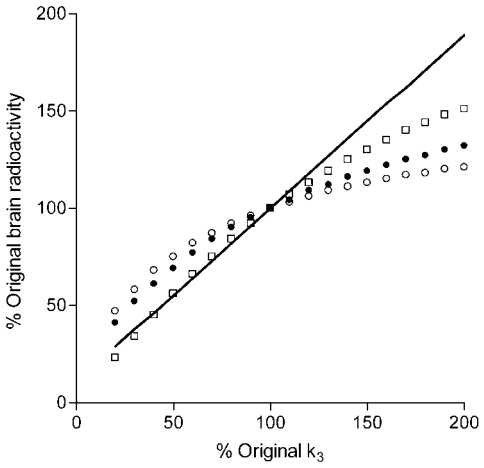

Figure 10. Simulated changes in brain uptake with variations of receptor density. Compared to V_T (shown by a line), brain uptake measured from 40 to 80 (○), 0 to 210 (●), and 150 to 180 (□) minutes is less sensitive to changes in k_3, which reflects receptor density.

This study demonstrated that [^{11}C]MePPEP is a suitable PET radioligand for imaging and quantifying CB_1 receptors in human brain. Our findings also support the use of compartment modeling as the "gold standard" to quantify receptor density, and that brain uptake uncorrected for parent radioligand in plasma is not appropriate for between subject comparisons. We found that precision of V_T was highly sensitive to variability from plasma measurements. In fact, we were limited not by brain measurements which we could collect throughout 10 half-lives of ^{11}C (due to the high uptake of [^{11}C]MePPEP in brain and PET camera sensitivity), but by low concentrations and radioactivity of [^{11}C]MePPEP in arterial plasma after 120 minutes.

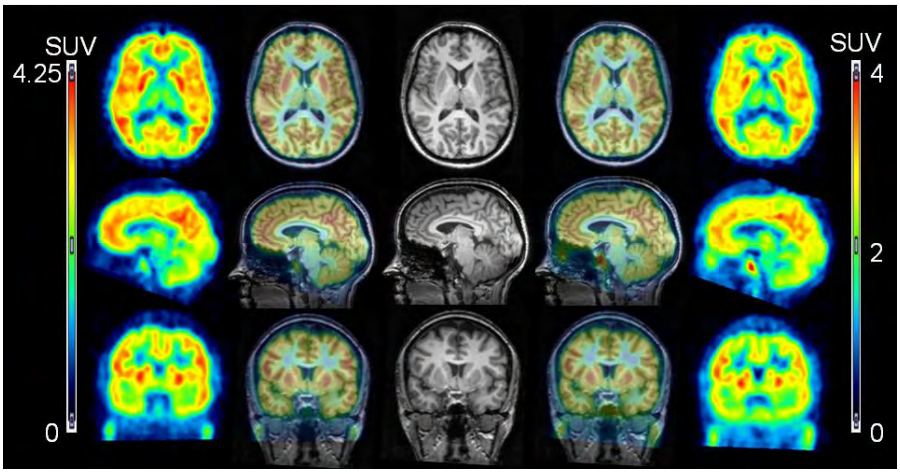

Figure 11. [^{11}C]MePPEP and [^{18}F]FMPEP-d_2 in human brain. PET images averaged from 40 to 80 minutes after injection of [^{11}C]MePPEP (far left column) and from 30 to 60 min after injection of [^{18}F]FMPEP-d_2 (far right column) and coregistered to the subject's MRI (middle column). PET and MR images are overlaid between their respective columns. All images are from the same subject. Standardized uptake value (SUV) corrects for body weight and injected radioactivity.

Therefore, we sought to evaluate a radioligand that would provide improved precision of plasma measurements, and improved accuracy of V_T.

IMAGING AND QUANTITATION OF CANNABINOID CB_1 RECEPTORS IN HUMAN AND MONKEY BRAIN USING ^{18}F-LABELED INVERSE AGONIST RADIOLIGANDS (PAPER III)

The simplest approach to developing a radioligand that would provide measureable concentrations of radioactivity for an extended time is to use a radionuclide with a longer radioactive half-life. Therefore, we evaluated three analogues of MePPEP labeled with ^{18}F ($t_{1/2}$ = 109.7 min; [^{18}F]FEPEP, [^{18}F]FMPEP, [^{18}F]FMPEP-d_2) and one labeled with ^{11}C ([^{11}C]FMePPEP), all of which were developed by a fellow graduate student at Karolinska Institutet and the National Institute of Mental Health[142,161]. These analogues were all structurally similar to MePPEP, with similar lipophilicities and higher binding affinities. Since we had thoroughly evaluated [^{11}C]MePPEP in rodents, monkeys, and humans, we briefly evaluated these novel radioligands in monkey brain and chose the best one to proceed to human studies.

We performed compartmental modeling in monkeys before and after blocking CB_1 receptors with rimonabant to find the amount of specific binding achieved by each radioligand. We found that [^{11}C]FMePPEP and [^{18}F]FEPEP had less than 73% specific binding, whereas [^{18}F]FMPEP had greater than 90% specific binding. Unfortunately [^{18}F]FMPEP also demonstrated a high amount of radioactivity uptake in bone as well, presumably due to free [^{18}F]fluoride which was formed as a metabolite from the parent radioligand. To reduce the formation of this troublesome metabolite which could confound PET measurements in brain, we developed [^{18}F]FMPEP-d_2. The replacement of the fluoromethoxy group with the dideuterofluoromethoxy group has been previously shown to reduce the *in vivo* production of [^{18}F]fluoride[162], and in fact we

found that [^{18}F]FMPEP-d_2 resulted in about 1/3 less radioactivity up take in bone than [^{18}F]FMPEP. We also found that the specific binding of [^{18}F]FMPEP-d_2 was nearly 90%, and that V_T could be stably identified within 90 minutes. Therefore we proceeded with [^{18}F]FMPEP-d_2 in humans.

We conducted retest studies using [^{18}F]FMPEP-d_2 to evaluate the precision of plasma measurements and accuracy of V_T. Similar to [^{11}C]MePPEP, [^{18}F]FMPEP-d_2 yielded high concentrations of radioactivity in areas of brain with high CB_1 receptor density within 20 to 60 minutes after injection (Fig. 11), with a similar between subject variability. However, [^{18}F]FMPEP-d_2 demonstrated a much better retest variability of plasma measurements (16%). This increased precision of plasma measurements led to a much reduced intersubject variability of V_T (26%), and, in conjunction with an extremely good ICC (0.89), suggests an improved accuracy of V_T. The impact of this improved accuracy was demonstrated in our simulations predicting the number of subjects required to detect changes in CB_1 receptor density, as we had done with [^{11}C]MePPEP. We found that V_T was superior to brain uptake in detecting either a 50% increase in receptor density (7 *vs.* 39 subjects required) or a 50% decrease in receptor density (7 *vs.* 12 subjects required).

A limitation that we encountered with [^{18}F]FMPEP-d_2 was an increasing value of V_T after 120 minutes (Fig. 12). Such a trend is consistent with an accumulation of radioactive metabolites in brain. We had also noted that radioactivity had accumulated in bone during the same time period, and wondered if that was the cause for our increase in V_T over time. To address this concern we created a conservative simulation predicting the contribution that radioactivity from the bone would contaminate measurements from brain and found that the amount was too small to be of practical consideration (<2%). Fortunately, V_T was measured with consistent and stable values from 60 to 120 minutes after injection, and therefore limiting scans to 120 minutes should avoid confounding changes to the accuracy of V_T.

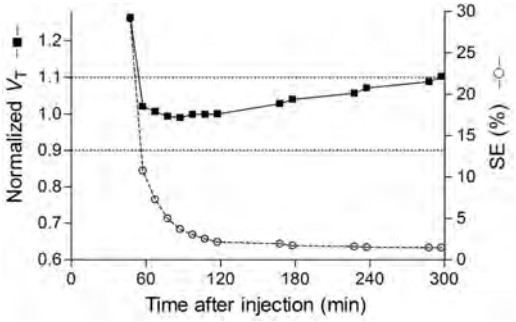

Figure 12. Distribution volume (V_T) of putamen and its identifiability as function of image acquisition time. V_T (■) was normalized to the value determined from 120 minutes of imaging and plotted with the *y*-axis on left. The corresponding SE (○), which is inversely proportional to identifiability, is plotted with the *y*-axis on right. V_T was stably identified between 60 and 120 min but gradually increased thereafter.

The plasma free fraction of both [^{11}C]MePPEP and [^{18}F]FMPEP-d_2 in human was very low (approximately 0.05% and 0.63%, respectively). The retest variability was excellent; however the intersubject variability was quite large. We suspect this was partly due to the nature of such low values, since small differences would be disproportionately large in percentage. Nevertheless, we found including free fraction in our analysis actually decreased the precision and accuracy of our outcome measurements. While correcting our measurements for free fraction would be

technically correct, we decided it added too much noise to our measurements to be considered in practice. Still, a low free fraction would be expected to have consequences as to the amount of radioligand available to enter brain in the case of a pharmacological challenge, as a proportionately large amount of radioligand could be displaced from plasma proteins and made available to enter brain.

This study demonstrated that [^{18}F]FMPEP-d_2 can provide robust measurements of CB_1 receptor density as V_T. We observed that increased precision of plasma measurements led to an increased accuracy of V_T, and that [^{18}F]FMPEP-d_2 has greater precision and accuracy than [^{11}C]MePPEP (Table 2). As such, [^{18}F]FMPEP-d_2 will require smaller sample sizes than [^{11}C]MePPEP to detect significant differences between groups (*e.g.*, patients *vs*. healthy subjects). Therefore, we suggest using [^{18}F]FMPEP-d_2 for future clinical studies measuring CB_1 receptor density.

Table 2. Comparison of [^{11}C]MePPEP and [^{18}F]FMPEP-d_2

	[^{11}C]MePPEP	[^{18}F]FMPEP-d_2
Distribution Volume		
V_T (mL • cm^{-3})	12 - 29	13 - 24
Intersubject variability	**> 50%**	**26%**
Retest variability	15%	14%
Brain uptake		
Peak in putamen (SUV)	3 - 4	3 - 4
Intersubject variability	16%	14%
Retest variability	8%	16%
Plasma $AUC_{0-\infty}$		
Intersubject variability	**>200%**	**0.13**
Retest variability	**58%**	**16%**
Radiation Dose		
Effective dose (μSv/MBq)	4.6	19.7
Intersubject variability	(n = 17)	(n = 8)
Retest variability	(n = 8)	(n = 9)

Three striking differences are highlighted in bold. The intersubject variability of V_T, and the intersubject and retest variability of plasma AUC [^{11}C]MePPEP are much higher than those of [^{18}F]FMPEP-d_2.

BIODISTRIBUTION AND DOSIMETRY IN HUMANS OF TWO INVERSE AGONISTS TO IMAGE CANNABINOID CB_1 RECEPTORS USING PET (PAPER IV)

Clinical PET studies have an associated radiation burden that can impact the amount of radioactivity used per study, and the number of studies that can be safely performed in a year. The radiation exposure from a PET study is dependent on the radioisotope and the biodistribution of the radioligand in the body. As a radioligand distributes in the body it will accumulate in some organs, where radiation will be both absorbed and emitted to neighboring organs. This process impacts the amount of radiation a given organ will receive, and could restrict the amount of radioligand that can be safely

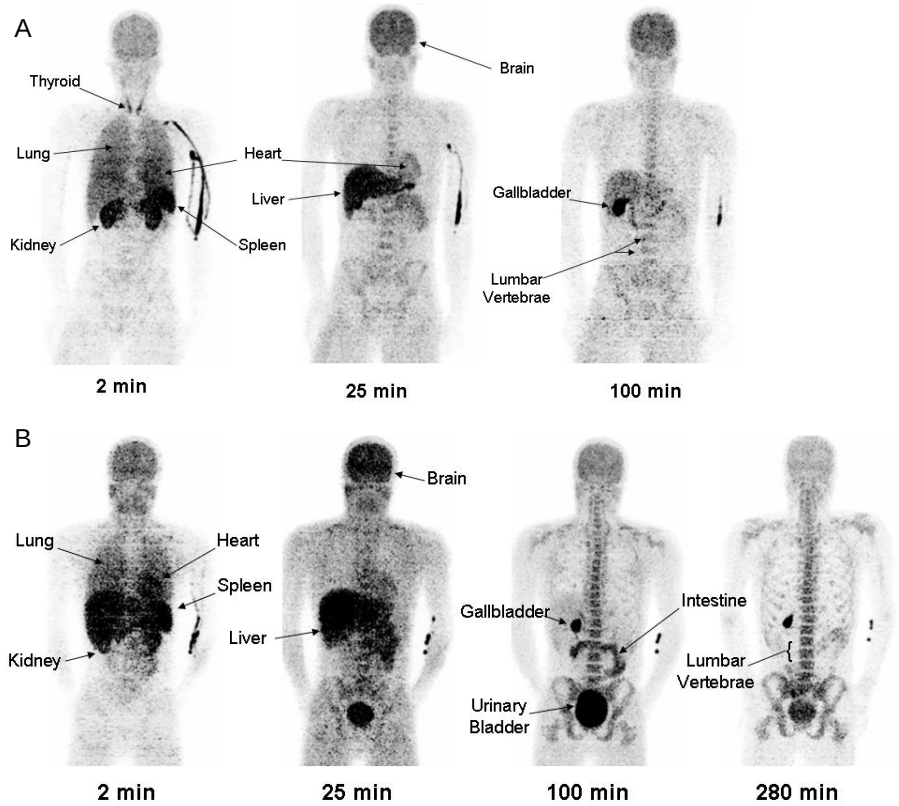

Figure 13. Biodistribution of A) [^{11}C]MePPEP and B) [^{18}F]FMPEP-d_2 in human at several times after injeciton of radioligand.

administered during a study. Therefore, it is important to understand the biodistribution of PET radioligands and to estimate the anticipated radiation exposure during a typical PET study.

We performed whole-body imaging studies with [^{11}C]MePPEP and [^{18}F]FMPEP-d_2 and observed the distribution and elimination of the radioligands. Both radioligands demonstrated high uptake of radioactivity in liver, lungs, and brain, and to a lesser extent in kidneys, heart, and spleen (Fig. 13). The majority of radioactivity in liver was likely due to parent radioligand that was metabolized and excreted in bile, as radioactivity accumulated in the gallbladder and was subsequently emptied into the small intestine. This appeared to be the only method of excretion for radioactivity from [^{11}C]MePPEP, while radioactivity from [^{18}F]FMPEP-d_2 also accumulated in the urinary bladder and was collected in voided urine. By modeling the amount of radioactivity collected from urine over time we estimated that about 33% of radioactivity from [^{18}F]FMPEP-d_2 was excereted in urine.

We observed accumulation of radioactivity in bone marrow in studies of both radioligands. The pattern of radioactivity accumulation in bone was consistent with areas rich in bone marrow, such as vertebrae, pelvis, and ribs. We confirmed that

radioactivity was not largely due to accumulation in bone itself by measuring radioactivity in bones devoid of bone marrow. Those bones had very little radioactivity compared to bones rich in bone marrow. We suspect that some of the uptake in red marrow is specific to CB_1 receptors present there, as monkeys demonstrated about 20% specific binding when compared before and after dosing with rimonabant (unpublished data).

The effective doses (*i.e.*, overall radiation doses) of [^{11}C]MePPEP and [^{18}F]FMPEP-d_2 are similar to other ^{11}C and ^{18}F-labeled radioligands. Thus, these radioligands could be used multiple times per year in an individual in a clinical setting. Our analysis of biodistribution also revealed that these radioligands have high proportional uptake in brain (8 – 10%) compared to other radioligands used for brain imaging, and are primarily cleared through the liver. The uptake of the radioligands in peripheral tissues with CB_1 receptors (liver, bone marrow, heart) suggest that they may be useful for imaging organs other than the brain or in diseases marked by CB_1 receptor overexpression (*i.e.*, cancer), though additional studies are needed to address this possibility.

CONCLUSIONS

The studies enclosed in this thesis have shown that [^{11}C]MePPEP and [^{18}F]FMPEP-d_2 have high specificity for CB_1 receptors, can be displaced by another inverse agonist, and can be quantified as distribution volume (V_T), an index of receptor density. To date, these are the only radioligands for CB_1 receptors for which full kinetic modeling data has been reported. In addition, we found that [^{11}C]MePPEP is not a substrate for the P-gp efflux transporter, and that it could not be displaced by endogenous or synthetic agonists. Therefore, these PET tracers should only be used for measuring changes or differences in receptor density, or for measuring receptor occupancy by inverse agonists; they should not be used for measuring receptor occupancy by agonists or endocannabinoid tone. Finally, both [^{11}C]MePPEP and [^{18}F]FMPEP-d_2 have an estimated radiation dose similar to that of other PET radioligands, and can be used safely in the clinical setting.

We suggest the use [^{18}F]FMPEP-d_2 in scans no more than 120 minutes with intermittent sampling of arterial blood to measure the density of CB_1 receptors between patients and healthy controls. Studies involving pharmacological doses of drugs should include measurements of free fraction to rule out confounding effects of radioligand displacement from plasma proteins. While [^{18}F]FMPEP-d_2 is the preferred radioligand, [^{11}C]MePPEP may be used if multiple studies per day in the same subject is desired. We expect that these radioligands will add tremendous value to the investigation of CB_1 receptor physiology, and the role CB_1 receptors play in neurological, psychiatric, and metabolic diseases.

FUTURE PERSPECTIVES

CB_1 AGONIST RADIOTRACER

Recently, much interest has been paid toward development of agonist radioligands. Agonist radioligands demonstrate preference for the high affinity, or G-protein bound, state, and are highly susceptible to competition from endogenous agonists. For example, a radioligand for high affinity dopamine D_2 receptors, [^{11}C]MNPA, demonstrates nearly twice the amount of displacement from dopamine than an antagonist, such as [^{11}C]raclopride[163]. Results from paper 1 in this thesis suggest that inverse agonists may not be susceptible to displacement by endogenous agonists since a very small proportion of receptors may be in the high affinity state. Therefore, development of an agonist radiotracer may provide tremendous insight into the endocannabinoid system.

If an agonist radiotracer for the CB_1 receptor were developed, several experiments probing the endocannabinoid system could be conceived. First, displacement of the radioligand by endogenous agonist could occur after blocking FAAH, as performed in paper 1, to approximate the endocannabinoid tone. Additional studies blocking the endocannabinoid transporter, endocannabinoid carriers, MAGL, or COX-2 selectively or in combination, could estimate the relative activity and metabolism of anandamide and 2-AG in brain. Studies involving the stimulation or inhibition of primary neurotransmitters could also be performed to gauge the relative response of endocannabinoids in the neuromoldulatory process of GABA, glutamate, and dopamine.

Development of an agonist radiotracer is likely to be difficult. Most existing agonists do not have high selectivity for the CB_1 receptor. Indeed, one of the first attempts to develop a radioligand to image CB_1 receptors was [^{18}F]Δ^8-THC, however Δ^8-THC exhibits nearly equal selectivity for CB_1 and CB_2 receptors and has a prohibitively high lipophilicity. Very few CB_1 agonists have the moderate lipophilicity required for a PET tracer; a notable exception is the aminoalkylindole class of agonists, typified by WIN-55,212-2. Finally, the development of an agonist radioligand may face the complexities posed by partial agonism and functional selectivity, which may present the CB_1 receptor with altered binding conformations for agonists.

IMAGING OTHER TARGETS OF THE ENDOCANNABINOID SYSTEM

As we gain a better understanding of the endocannabinoid system and its components, new targets for PET radioligand development will emerge. Development of compounds that inhibit FAAH for use in pharmacotherapy is underway, as it may be useful in the treatment of diseases such as depression[164]. Therefore, a radioligand for FAAH would be useful, and several candidates have already been proposed[165]. Similarly, radioligands for the putative endocannabinoid transporter and MAG lipase would permit further investigation of their function. Candidates for imaging CB_2 receptors have already been developed[166], and a successful radioligand would be useful in the examining the role of CB_2 receptors in pain and inflammation. Currently, no PET radioligands have been

reported for GPR55 (a suspected cannabinoid receptor) or TRPV1 (a receptor to which anandamide binds), targets which could expand our understanding of the endocannabinoid system.

IMAGING THE ENDOCANNABINOID SYSTEM IN THE PERIPHERY

The focus of this thesis has been on the imaging and quantitation of CB_1 receptors in brain. However, several disease processes outside of the brain involve alterations in CB_1 receptor expression, and would therefore be candidates for imaging using a CB_1 receptor-selective PET tracer. For example, CB_1 receptors have been associated with liver cirrhosis, cardiovascular regulation, and certain types of cancers[61]. At present, insufficient data is available to determine if [^{11}C]MePPEP or [^{18}F]FMPEP-d_2 would be optimal for use in peripheral imaging of diseases, and what the optimal method of analysis would be for that analysis (radioactivity concentration *vs.* distribution volume). More research as to the appropriate use of these tracers for imaging CB_1 receptors outside the brain needs to be performed.

ACKNOWLEDGEMENTS

There are many people who have assisted in the projects described in this thesis, and there are many more who have encouraged and fostered my interests in PET. My gratitude and appreciation go out to all of them, and in particular I would like to thank:

My mentor Robert Innis, whose guidance and example has taught me so much about being a scientist, a careful analyst, and a writer.

My mentor Christer Halldin, whose insight, work ethic, and pointed questions have challenged me to continually improve.

The Molecular Imaging Branch (MIB), in particular:

Elizabeth Alzona, who provided an enormous amount support every day, guiding me through the inner workings of NIH.

Jussi Hirvonen, with whom I had endless discussions on analysis of precision and accuracy, limited only by my brain getting full.

Jeih-San Liow, who taught me so much about PET instrumentation and rodent work, who always challenged me with his curiosity, and whose friendship made the last several years pass too quickly.

Sami Zoghbi, whose meticulous attention to detail has often brought order to the chaos of plasma analysis.

Robert Gladding, for his help with the monkey studies, and whose humor and good nature provided good stress relief.

Chuck Kreisl, who provided clinical support and frequently offered himself as a sounding board for ideas.

Barbara Scepura, Desiree Ferraris Araneta, Gerald Hodges, and Janet Sangare, who provided clinical support for all of the human studies.

Amanda Farris and Leah Dickstein for their assistance in coordinating the human studies.

Ed Tuan, Pavitra Kannan, Kim Jenko, and Kacey Anderson who provided much appreciated support for radioligand analysis.

The radiochemistry section including Cheryl Morse, Sean Donohue, Jinsoo Hong, Yi Zhang, and led by Vic Pike, all of whose dedication to radioligand development and production helps to fuel the engine of research at MIB.

NIH PET department, the nursing staff of 5SW, and the NIMH veterinary staff who provided logistical support throughout this thesis.

Karin Zahir, who has helped me with everything from Swedish translation of food to the proofing of this thesis.

Nick Seneca, whose pioneering spirit in the NIMH-KI program laid the foundation for me and all other students who followed, and whose advice and friendship helped me from beginning to end.

My collaborators at Lilly Research Laboratories, Johannes Tauscher, John Schaus, Lee Phebus, Christian Felder, and Eyassu Chernet for their thoughtful support and direction throughout this project.

Eric Hostetler, who taught me the ways of the radiochemist, to constantly optimize methods and procedures, and with whom I've shared some good times and a good friendship.

Don Burns and Richard Hargreaves, who provided my first opportunity to get involved in PET research, and gave me a launching pad to continue my career; and the rest of the MRL Imaging Research lab, whose camaraderie made working there a pleasure.

Rachel Powsner, whose book "Essentials of Nuclear Medicine Physics" first brought PET to my attention and has sparked my career in PET and medical imaging.

My family: Mom and Dad, whose support and encouragement have fostered my pursuits in all arenas.
Katie and Beth, whose examples have paved the way for me to aim high.
Papa, who I believe first planted the seed of pursuing an MD/PhD degree years ago.

Kerin Hoag, whose support since the beginning of my PhD studies has been there in the best of times and worst of times.

Linda Werling, whose support and encouragement as external mentor helped me to maintain a good perspective on science, and to always stay curious.

My classmates in the NIH Graduate Partnership Program and the Karolinska Institutet, whose generosity has supported, and whose desire for betterment has enhanced, this unique program.

My classmates of the George Washington School of Medicine, whose drive and enthusiasm has made the experience a whole lot of fun.

The volunteers who participated in these studies.

The National Institutes of Health, the National Institute of Mental Health, the Office of the Director, and Karolinska Institutet for their financial support, and for the rich environment of scientific learning they provide, which has made this a stimulating experience.

REFERENCES

1. Copeland J, Swift W. (2009) Cannabis use disorder: epidemiology and management. *Int Rev Psychiatry* 21:96-103.
2. Howlett AC, Barth F, Bonner TI, Cabral G, Casellas P, Devane WA, Felder CC, Herkenham M, Mackie K, Martin BR, Mechoulam R, Pertwee RG. (2002) International Union of Pharmacology. XXVII. Classification of cannabinoid receptors. *Pharmacol Rev* 54:161-202.
3. Howlett AC. (2005) Cannabinoid receptor signaling. *Handb Exp Pharmacol*:53-79
4. Munro S, Thomas KL, Abu-Shaar M. (1993) Molecular characterization of a peripheral receptor for cannabinoids. *Nature* 365:61-65.
5. Abood ME. (2005) Molecular biology of cannabinoid receptors. *Handb Exp Pharmacol*:81-115.
6. McAllister SD, Rizvi G, Anavi-Goffer S, Hurst DP, Barnett-Norris J, Lynch DL, Reggio PH, Abood ME. (2003) An aromatic microdomain at the cannabinoid CB_1 receptor constitutes an agonist/inverse agonist binding region. *J Med Chem* 46:5139-5152.
7. Baker D, Pryce G, Davies WL, Hiley CR. (2006) In silico patent searching reveals a new cannabinoid receptor. *Trends Pharmacol Sci* 27:1-4.
8. Elphick MR, Egertova M. (2001) The neurobiology and evolution of cannabinoid signalling. *Philos Trans R Soc Lond B Biol Sci* 356:381-408.
9. McPartland JM, Glass M. (2003) Functional mapping of cannabinoid receptor homologs in mammals, other vertebrates, and invertebrates. *Gene* 312:297-303.
10. McPartland JM, Matias I, Di Marzo V, Glass M. (2006) Evolutionary origins of the endocannabinoid system. *Gene* 370:64-74.
11. Elphick MR, Egertova M. (2005) The phylogenetic distribution and evolutionary origins of endocannabinoid signalling. *Handb Exp Pharmacol*:283-297.
12. Zimmer A, Zimmer AM, Hohmann AG, Herkenham M, Bonner TI. (1999) Increased mortality, hypoactivity, and hypoalgesia in cannabinoid CB_1 receptor knockout mice. *Proc Natl Acad Sci U S A* 96:5780-5785.
13. Ledent C, Valverde O, Cossu G, Petitet F, Aubert JF, Beslot F, Bohme GA, Imperato A, Pedrazzini T, Roques BP, Vassart G, Fratta W, Parmentier M. (1999) Unresponsiveness to cannabinoids and reduced addictive effects of opiates in CB_1 receptor knockout mice. *Science* 283:401-404.
14. Hoehe MR, Caenazzo L, Martinez MM, Hsieh WT, Modi WS, Gershon ES, Bonner TI. (1991) Genetic and physical mapping of the human cannabinoid receptor gene to chromosome 6q14-q15. *New Biol* 3:880-885.
15. Shire D, Carillon C, Kaghad M, Calandra B, Rinaldi-Carmona M, Le Fur G, Caput D, Ferrara P. (1995) An amino-terminal variant of the central cannabinoid receptor resulting from alternative splicing. *J Biol Chem* 270:3726-3731.
16. Juhasz G, Chase D, Pegg E, Downey D, Toth ZG, Stones K, Platt H, Mekli K, Payton A, Elliott R, Anderson IM, Deakin JF. (2009) CNR1 gene is associated with high neuroticism and low agreeableness and interacts with recent negative life events to predict current depressive symptoms. *Neuropsychopharmacology* 34:2019-2027.

17. Benzinou M, Chevre JC, Ward KJ, Lecoeur C, Dina C, Lobbens S, Durand E, Delplanque J, Horber FF, Heude B, Balkau B, Borch-Johnsen K, Jorgensen T, Hansen T, Pedersen O, Meyre D, Froguel P. (2008) Endocannabinoid receptor 1 gene variations increase risk for obesity and modulate body mass index in European populations. *Hum Mol Genet* 17:1916-1921.
18. Chakrabarti A, Onaivi ES, Chaudhuri G. (1995) Cloning and sequencing of a cDNA encoding the mouse brain-type cannabinoid receptor protein. *DNA Seq* 5:385-388
19. Abood ME, Ditto KE, Noel MA, Showalter VM, Tao Q. (1997) Isolation and expression of a mouse CB_1 cannabinoid receptor gene. Comparison of binding properties with those of native CB_1 receptors in mouse brain and N18TG2 neuroblastoma cells. *Biochem Pharmacol* 53:207-214.
20. Hirst RA, Almond SL, Lambert DG. (1996) Characterisation of the rat cerebella CB_1 receptor using SR141716A, a central cannabinoid receptor antagonist. *Neurosci Lett* 220:101-104.
21. Herkenham M, Lynn AB, Little MD, Johnson MR, Melvin LS, de Costa BR, Rice KC. (1990) Cannabinoid receptor localization in brain. *Proc Natl Acad Sci U S A* 87:1932-1936.
22. Glass M, Dragunow M, Faull RL. (1997) Cannabinoid receptors in the human brain: a detailed anatomical and quantitative autoradiographic study in the fetal, neonatal and adult human brain. *Neuroscience* 77:299-318.
23. Ramirez BG, Blazquez C, Gomez del Pulgar T, Guzman M, de Ceballos ML. (2005) Prevention of Alzheimer's disease pathology by cannabinoids: neuroprotection mediated by blockade of microglial activation. *J Neurosci* 25:1904-1913.
24. Galiegue S, Mary S, Marchand J, Dussossoy D, Carriere D, Carayon P, Bouaboula M, Shire D, Le Fur G, Casellas P. (1995) Expression of central and peripheral cannabinoid receptors in human immune tissues and leukocyte subpopulations. *Eur J Biochem* 232:54-61.
25. Gaoni Y, Mechoulam R. (1964) Hashish. III. Isolation, structure, and partial synthesis of an active constituent of hashish. *J Am Chem Soc* 86:1646-1647.
26. Mechoulam R, Gaoni Y. (1967) The absolute configuration of delta-1-tetrahydrocannabinol, the major active constituent of hashish. *Tetrahedron Lett* 12:1109-1111.
27. Jones G, Pertwee RG, Gill EW, Paton WD, Nilsson IM, Widman M, Agurell S. (1974) Relative pharmacological potency in mice of optical isomers of delta 1-tetrahydrocannabinol. *Biochem Pharmacol* 23:439-446.
28. Matsuda LA, Lolait SJ, Brownstein MJ, Young AC, Bonner TI. (1990) Structure of a cannabinoid receptor and functional expression of the cloned cDNA. *Nature* 346:561-564.
29. Devane WA, Hanus L, Breuer A, Pertwee RG, Stevenson LA, Griffin G, Gibson D, Mandelbaum A, Etinger A, Mechoulam R. (1992) Isolation and structure of a brain constituent that binds to the cannabinoid receptor. *Science* 258:1946-1949.
30. Stella N, Schweitzer P, Piomelli D. (1997) A second endogenous cannabinoid that modulates long-term potentiation. *Nature* 388:773-778.
31. Bisogno T, Melck D, Bobrov M, Gretskaya NM, Bezuglov VV, De Petrocellis L, Di Marzo V. (2000) N-acyl-dopamines: novel synthetic CB(1) cannabinoid-receptor ligands and inhibitors of anandamide inactivation

with cannabimimetic activity in vitro and in vivo. *Biochem J* 351 Pt 3:817-824.

32. Hanus L, Abu-Lafi S, Fride E, Breuer A, Vogel Z, Shalev DE, Kustanovich I, Mechoulam R. (2001) 2-arachidonyl glyceryl ether, an endogenous agonist of the cannabinoid CB_1 receptor. *Proc Natl Acad Sci U S A* 98:3662-3665.
33. Porter AC, Sauer JM, Knierman MD, Becker GW, Berna MJ, Bao J, Nomikos GG, Carter P, Bymaster FP, Leese AB, Felder CC. (2002) Characterization of a novel endocannabinoid, virodhamine, with antagonist activity at the CB_1 receptor. *J Pharmacol Exp Ther* 301:1020-1024.
34. Balvers MG, Verhoeckx KC, Witkamp RF. (2009) Development and validation of a quantitative method for the determination of 12 endocannabinoids and related compounds in human plasma using liquid chromatography-tandem mass spectrometry. *J Chromatogr B Analyt Technol Biomed Life Sci* 877:1583-1590.
35. Glass M, Northup JK. (1999) Agonist selective regulation of G proteins by cannabinoid CB(1) and CB(2) receptors. *Mol Pharmacol* 56:1362-1369.
36. Georgieva T, Devanathan S, Stropova D, Park CK, Salamon Z, Tollin G, Hruby VJ, Roeske WR, Yamamura HI, Varga E. (2008) Unique agonist-bound cannabinoid CB_1 receptor conformations indicate agonist specificity in signaling. *Eur J Pharmacol* 581:19-29.
37. Thakur GA, Nikas SP, Li C, Makriyannis A. (2005) Structural requirements for cannabinoid receptor probes. *Handb Exp Pharmacol*:209-246.
38. Burkey TH, Quock RM, Consroe P, Ehlert FJ, Hosohata Y, Roeske WR, Yamamura HI. (1997) Relative efficacies of cannabinoid CB_1 receptor agonists in the mouse brain. *Eur J Pharmacol* 336:295-298.
39. Bell MR, D'Ambra TE, Kumar V, Eissenstat MA, Herrmann JL, Jr., Wetzel JR, Rosi D, Philion RE, Daum SJ, Hlasta DJ, et al. (1991) Antinociceptive (aminoalkyl)indoles. *J Med Chem* 34:1099-1110.
40. Rinaldi-Carmona M, Barth F, Heaulme M, Shire D, Calandra B, Congy C, Martinez S, Maruani J, Neliat G, Caput D, et al. (1994) SR141716A, a potent and selective antagonist of the brain cannabinoid receptor. *FEBS Lett* 350:240-244.
41. Kenakin T. (2001) Inverse, protean, and ligand-selective agonism: matters of receptor conformation. *Faseb J* 15:598-611.
42. Pertwee RG. (2005) Inverse agonism and neutral antagonism at cannabinoid CB_1 receptors. *Life Sci* 76:1307-1324.
43. Okamoto Y, Morishita J, Tsuboi K, Tonai T, Ueda N. (2004) Molecular characterization of a phospholipase D generating anandamide and its congeners. *J Biol Chem* 279:5298-5305.
44. Simon GM, Cravatt BF. (2006) Endocannabinoid biosynthesis proceeding through glycerophospho-N-acyl ethanolamine and a role for alpha/beta-hydrolase 4 in this pathway. *J Biol Chem* 281:26465-26472.
45. Liu J, Wang L, Harvey-White J, Osei-Hyiaman D, Razdan R, Gong Q, Chan AC, Zhou Z, Huang BX, Kim HY, Kunos G. (2006) A biosynthetic pathway for anandamide. *Proc Natl Acad Sci U S A* 103:13345-13350.
46. Bisogno T, Howell F, Williams G, Minassi A, Cascio MG, Ligresti A, Matias I, Schiano-Moriello A, Paul P, Williams EJ, Gangadharan U, Hobbs C, Di Marzo V, Doherty P. (2003) Cloning of the first sn1-DAG lipases points

to the spatial and temporal regulation of endocannabinoid signaling in the brain. *J Cell Biol* 163:463-468.

47. Hill MN, McEwen BS. (2009) Endocannabinoids: The silent partner of glucocorticoids in the synapse. *Proc Natl Acad Sci U S A* 106:4579-4580.
48. Zhao P, Leonoudakis D, Abood ME, Beattie EC. (2009) Cannabinoid receptor activation reduces TNFalpha-Induced surface localization of AMPAR-type glutamate receptors and excitotoxicity. *Neuropharmacology* In press.
49. Sun Y, Alexander SP, Kendall DA, Bennett AJ. (2006) Cannabinoids and PPARalpha signalling. *Biochem Soc Trans* 34:1095-1097.
50. Riedel G, Davies SN. (2005) Cannabinoid function in learning, memory and plasticity. *Handb Exp Pharmacol*:445-477.
51. Chhatwal JP, Davis M, Maguschak KA, Ressler KJ. (2005) Enhancing cannabinoid neurotransmission augments the extinction of conditioned fear. *Neuropsychopharmacology* 30:516-524.
52. Felder CC, Dickason-Chesterfield AK, Moore SA. (2006) Cannabinoids biology: the search for new therapeutic targets. *Mol Interv* 6:149-161.
53. Kaczocha M, Glaser ST, Deutsch DG. (2009) Identification of intracellular carriers for the endocannabinoid anandamide. *Proc Natl Acad Sci U S A* 106:6375-6380.
54. Cravatt BF, Giang DK, Mayfield SP, Boger DL, Lerner RA, Gilula NB. (1996) Molecular characterization of an enzyme that degrades neuromodulatory fatty-acid amides. *Nature* 384:83-87.
55. Wei BQ, Mikkelsen TS, McKinney MK, Lander ES, Cravatt BF. (2006) A second fatty acid amide hydrolase with variable distribution among placental mammals. *J Biol Chem* 281:36569-36578.
56. Egertova M, Giang DK, Cravatt BF, Elphick MR. (1998) A new perspective on cannabinoid signalling: complementary localization of fatty acid amide hydrolase and the CB_1 receptor in rat brain. *Proc Biol Sci* 265:2081-2085.
57. Tsuboi K, Sun YX, Okamoto Y, Araki N, Tonai T, Ueda N. (2005) Molecular characterization of N-acylethanolamine-hydrolyzing acid amidase, a novel member of the choloylglycine hydrolase family with structural and functional similarity to acid ceramidase. *J Biol Chem* 280:11082-11092.
58. Dinh TP, Carpenter D, Leslie FM, Freund TF, Katona I, Sensi SL, Kathuria S, Piomelli D. (2002) Brain monoglyceride lipase participating in endocannabinoid inactivation. *Proc Natl Acad Sci U S A* 99:10819-10824.
59. Kozak KR, Crews BC, Morrow JD, Wang LH, Ma YH, Weinander R, Jakobsson PJ, Marnett LJ. (2002) Metabolism of the endocannabinoids, 2-arachidonylglycerol and anandamide, into prostaglandin, thromboxane, and prostacyclin glycerol esters and ethanolamides. *J Biol Chem* 277:44877-44885.
60. Woodward DF, Carling RW, Cornell CL, Fliri HG, Martos JL, Pettit SN, Liang Y, Wang JW. (2008) The pharmacology and therapeutic relevance of endocannabinoid derived cyclo-oxygenase (COX)-2 products. *Pharmacol Ther* 120:71-80.
61. Pacher P, Batkai S, Kunos G. (2006) The endocannabinoid system as an emerging target of pharmacotherapy. *Pharmacol Rev* 58:389-462.
62. Ashton H, Golding J, Marsh VR, Millman JE, Thompson JW. (1981) The seed and the soil: effect of dosage, personality and starting state on the response to delta 9 tetrahydrocannabinol in man. *Br J Clin Pharmacol* 12:705-720.

63. Piomelli D. (2003) The molecular logic of endocannabinoid signalling. *Nat Rev Neurosci* 4:873-884.
64. Hill EL, Gallopin T, Ferezou I, Cauli B, Rossier J, Schweitzer P, Lambolez B. (2007) Functional CB_1 receptors are broadly expressed in neocortical GABAergic and glutamatergic neurons. *J Neurophysiol* 97:2580-2589.
65. Hill MN, Gorzalka BB. (2005) Is there a role for the endocannabinoid system in the etiology and treatment of melancholic depression? *Behav Pharmacol* 16:333-352.
66. Basavarajappa BS. (2007) The endocannabinoid signaling system: a potential target for next-generation therapeutics for alcoholism. *Mini Rev Med Chem* 7:769-779.
67. Lopez-Moreno JA, Gonzalez-Cuevas G, Moreno G, Navarro M. (2008) The pharmacology of the endocannabinoid system: functional and structural interactions with other neurotransmitter systems and their repercussions in behavioral addiction. *Addict Biol* 13:160-187.
68. D'Souza DC, Perry E, MacDougall L, Ammerman Y, Cooper T, Wu YT, Braley G, Gueorguieva R, Krystal JH. (2004) The psychotomimetic effects of intravenous delta-9-tetrahydrocannabinol in healthy individuals: implications for psychosis. *Neuropsychopharmacology* 29:1558-1572.
69. Caspi A, Moffitt TE, Cannon M, McClay J, Murray R, Harrington H, Taylor A, Arseneault L, Williams B, Braithwaite A, Poulton R, Craig IW. (2005) Moderation of the effect of adolescent-onset cannabis use on adult psychosis by a functional polymorphism in the catechol-O-methyltransferase gene: longitudinal evidence of a gene X environment interaction. *Biol Psychiatry* 57:1117-1127.
70. Sugranyes G, Flamarique I, Parellada E, Baeza I, Goti J, Fernandez-Egea E, Bernardo M. (2009) Cannabis use and age of diagnosis of schizophrenia. *Eur Psychiatry* 24:282-286.
71. Fernandez-Espejo E, Viveros MP, Nunez L, Ellenbroek BA, Rodriguez de Fonseca F. (2009) Role of cannabis and endocannabinoids in the genesis of schizophrenia. *Psychopharmacology (Berl)* 206:531-549.
72. Orgado JM, Fernandez-Ruiz J, Romero J. (2009) The endocannabinoid system in neuropathological states. *Int Rev Psychiatry* 21:172-180.
73. Allen KL, Waldvogel HJ, Glass M, Faull RL. (2009) Cannabinoid (CB_1), GABA(A) and GABA(B) receptor subunit changes in the globus pallidus in Huntington's disease. *J Chem Neuroanat* 37:266-281.
74. Monory K, Massa F, Egertova M, Eder M, Blaudzun H, Westenbroek R, Kelsch W, Jacob W, Marsch R, Ekker M, Long J, Rubenstein JL, Goebbels S, Nave KA, During M, Klugmann M, Wolfel B, Dodt HU, Zieglgansberger W, Wotjak CT, Mackie K, Elphick MR, Marsicano G, Lutz B. (2006) The endocannabinoid system controls key epileptogenic circuits in the hippocampus. *Neuron* 51:455-466.
75. Ludanyi A, Eross L, Czirjak S, Vajda J, Halasz P, Watanabe M, Palkovits M, Magloczky Z, Freund TF, Katona I. (2008) Downregulation of the CB_1 cannabinoid receptor and related molecular elements of the endocannabinoid system in epileptic human hippocampus. *J Neurosci* 28:2976-2990.
76. Nogueiras R, Veyrat-Durebex C, Suchanek PM, Klein M, Tschop J, Caldwell C, Woods SC, Wittmann G, Watanabe M, Liposits Z, Fekete C, Reizes O, Rohner-Jeanrenaud F, Tschop MH. (2008) Peripheral, but not central,

CB_1 antagonism provides food intake-independent metabolic benefits in diet-induced obese rats. *Diabetes* 57:2977-2991.

77. Jbilo O, Ravinet-Trillou C, Arnone M, Buisson I, Bribes E, Peleraux A, Penarier G, Soubrie P, Le Fur G, Galiegue S, Casellas P. (2005) The CB_1 receptor antagonist rimonabant reverses the diet-induced obesity phenotype through the regulation of lipolysis and energy balance. *Faseb J* 19:1567-1569.
78. Benzinou M, Chevre JC, Ward KJ, Lecoeur C, Dina C, Lobbens S, Durand E, Delplanque J, Horber FF, Heude B, Balkau B, Borch-Johnsen K, Jorgensen T, Hansen T, Pedersen O, Meyre D, Froguel P. (2008) Endocannabinoid receptor 1 gene variations increase risk for obesity and modulate body mass index in European populations. *Hum Mol Genet* 17:1916-1921.
79. Hayakawa K, Mishima K, Nozako M, Hazekawa M, Aoyama Y, Ogata A, Harada K, Fujioka M, Abe K, Egashira N, Iwasaki K, Fujiwara M. (2007) High-cholesterol feeding aggravates cerebral infarction via decreasing the CB_1 receptor. *Neurosci Lett* 414:183-187.
80. Booth M. (2003) *Cannabis*. New York: St. Martin's Press.
81. Iverson L. (2008) *The Science of Marijuana*. Oxford: Oxford University Press.
82. Van Gaal LF, Rissanen AM, Scheen AJ, Ziegler O, Rossner S. (2005) Effects of the cannabinoid-1 receptor blocker rimonabant on weight reduction and cardiovascular risk factors in overweight patients: 1-year experience from the RIO-Europe study. *Lancet* 365:1389-1397.
83. Pi-Sunyer FX, Aronne LJ, Heshmati HM, Devin J, Rosenstock J. (2006) Effect of rimonabant, a cannabinoid-1 receptor blocker, on weight and cardiometabolic risk factors in overweight or obese patients: RIO-North America: a randomized controlled trial. *Jama* 295:761-775.
84. Rosenstock J, Hollander P, Chevalier S, Iranmanesh A. (2008) SERENADE: the Study Evaluating Rimonabant Efficacy in Drug-naive Diabetic Patients: effects of monotherapy with rimonabant, the first selective CB_1 receptor antagonist, on glycemic control, body weight, and lipid profile in drug-naive type 2 diabetes. *Diabetes Care* 31:2169-2176.
85. Despres JP, Ross R, Boka G, Almeras N, Lemieux I. (2009) Effect of rimonabant on the high-triglyceride/ low-HDL-cholesterol dyslipidemia, intraabdominal adiposity, and liver fat: the ADAGIO-Lipids trial. *Arterioscler Thromb Vasc Biol* 29:416-423.
86. Nissen SE, Nicholls SJ, Wolski K, Rodes-Cabau J, Cannon CP, Deanfield JE, Despres JP, Kastelein JJ, Steinhubl SR, Kapadia S, Yasin M, Ruzyllo W, Gaudin C, Job B, Hu B, Bhatt DL, Lincoff AM, Tuzcu EM. (2008) Effect of rimonabant on progression of atherosclerosis in patients with abdominal obesity and coronary artery disease: the STRADIVARIUS randomized controlled trial. *Jama* 299:1547-1560.
87. Soyka M, Koller G, Schmidt P, Lesch OM, Leweke M, Fehr C, Gann H, Mann KF. (2008) Cannabinoid receptor 1 blocker rimonabant (SR 141716) for treatment of alcohol dependence: results from a placebo-controlled, double-blind trial. *J Clin Psychopharmacol* 28:317-324.
88. Cahill K, Ussher M. (2007) Cannabinoid type 1 receptor antagonists (rimonabant) for smoking cessation. *Cochrane Database Syst Rev*:CD005353.
89. Jones D. (2008) End of the line for cannabinoid receptor 1 as an anti-obesity target? *Nat Rev Drug Discov* 7:961-962.

90. Le Foll B, Gorelick DA, Goldberg SR. (2009) The future of endocannabinoid-oriented clinical research after CB_1 antagonists. *Psychopharmacology (Berl)* 205:171-174.
91. Kunos G, Osei-Hyiaman D, Batkai S, Sharkey KA, Makriyannis A. (2009) Should peripheral CB_1 cannabinoid receptors be selectively targeted for therapeutic gain? *Trends Pharmacol Sci* 30:1-7.
92. McElroy J, Sieracki K, Chorvat R. (2008) Non-Brain-Penetrant CB_1 Receptor Antagonists as a Novel Treatment of Obesity and Related Metabolic Disorders. *Obesity* 16:S47.
93. Piomelli D, Tarzia G, Duranti A, Tontini A, Mor M, Compton TR, Dasse O, Monaghan EP, Parrott JA, Putman D. (2006) Pharmacological profile of the selective FAAH inhibitor KDS-4103 (URB597). *CNS Drug Rev* 12:21-38.
94. Hogestatt ED, Jonsson BA, Ermund A, Andersson DA, Bjork H, Alexander JP, Cravatt BF, Basbaum AI, Zygmunt PM. (2005) Conversion of acetaminophen to the bioactive N-acylphenolamine AM404 via fatty acid amide hydrolase-dependent arachidonic acid conjugation in the nervous system. *J Biol Chem* 280:31405-31412.
95. La Rana G, Russo R, Campolongo P, Bortolato M, Mangieri RA, Cuomo V, Iacono A, Raso GM, Meli R, Piomelli D, Calignano A. (2006) Modulation of neuropathic and inflammatory pain by the endocannabinoid transport inhibitor AM404 [N-(4-hydroxyphenyl)-eicosa-5,8,11,14-tetraenamide]. *J Pharmacol Exp Ther* 317:1365-1371.
96. Phelps ME. (1991) PET: a biological imaging technique. *Neurochem Res* 16:929-940.
97. Smith GS, Koppel J, Goldberg S. (2003) Applications of neuroreceptor imaging to psychiatry research. *Psychopharmacol Bull* 37:26-65.
98. Lee CM, Farde L. (2006) Using positron emission tomography to facilitate CNS drug development. *Trends Pharmacol Sci* 27:310-316.
99. Hargreaves RJ. (2008) The role of molecular imaging in drug discovery and development. *Clin Pharmacol Ther* 83:349-353.
100. Fujita M, Kugaya A, Innis RB. (2005) Radiotracer Imaging: Basic Principles and Exemplary Findings in Neuropsychiatric Disorders. In: *In Comprehensive Textbook of Psychiatry* (Kaplan HI, Sadock BJ, eds), Baltimore, MD: Williams and Wilkins, pp 222-235.
101. Shiue CY, Shiue GG, Cornish KG, O'Rourke MF. (1995) PET study of the distribution of [^{11}C]fluoxetine in a monkey brain. *Nucl Med Biol* 22:613-616.
102. Halldin C, Gulyas B, Farde L. (2001) PET studies with carbon-11 radioligands in neuropsychopharmacological drug development. *Curr Pharm Des* 7:1907-1929.
103. Kegeles LS, Mann JJ. (1997) In vivo imaging of neurotransmitter systems using radiolabeled receptor ligands. *Neuropsychopharmacology* 17:293-307.
104. Pike VW, Halldin C, Crouzel C, Barre L, Nutt DJ, Osman S, Shah F, Turton DR, Waters SL. (1993) Radioligands for PET studies of central benzodiazepine receptors and PK (peripheral benzodiazepine) binding sites--current status. *Nucl Med Biol* 20:503-525.
105. Bonhomme-Faivre L, Benyamina A, Reynaud M, Farinotti R, Abbara C. (2008) Disposition of Delta tetrahydrocannabinol in CF1 mice deficient in mdr1a P-glycoprotein. *Addict Biol* 13:295-300.

106. Koeppe RA, Shulkin BL, Rosenspire KC, Shaw LA, Betz AL, Mangner T, Price JC, Agranoff BW. (1991) Effect of aspartame-derived phenylalanine on neutral amino acid uptake in human brain: a positron emission tomography study. *J Neurochem* 56:1526-1535.
107. Innis RB, Cunningham VJ, Delforge J, Fujita M, Gjedde A, Gunn RN, Holden J, Houle S, Huang SC, Ichise M, Iida H, Ito H, Kimura Y, Koeppe RA, Knudsen GM, Knuuti J, Lammertsma AA, Laruelle M, Logan J, Maguire RP, Mintun MA, Morris ED, Parsey R, Price JC, Slifstein M, Sossi V, Suhara T, Votaw JR, Wong DF, Carson RE. (2007) Consensus nomenclature for in vivo imaging of reversibly binding radioligands. *J Cereb Blood Flow Metab* 27:1533-1539.
108. NIH Roadmap Working Group. (2004) NIH Roadmap: Reengineering the Clinical Research Enterprise. Retrieved October 6, 2009 from http://nihroadmap.nih.gov/clinicalresearch/rtrc/pdf/rtrc_interimreport.pdf
109. Cherry SR, Gambhir SS. (2001) Use of positron emission tomography in animal research. *ILAR J* 42:219-232.
110. Shetty HU, Zoghbi SS, Simeon FG, Liow JS, Brown AK, Kannan P, Innis RB, Pike VW. (2008) Radiodefluorination of 3-fluoro-5-(2-(2-[^{18}F](fluoromethyl)-thiazol-4-yl)ethynyl)benzonitrile ([^{18}F]SP203), a radioligand for imaging brain metabotropic glutamate subtype-5 receptors with positron emission tomography, occurs by glutathionylation in rat brain. *J Pharmacol Exp Ther* 327:727-735.
111. Brown AK, Kimura Y, Zoghbi SS, Simeon FG, Liow JS, Kreisl WC, Taku A, Fujita M, Pike VW, Innis RB. (2008) Metabotropic glutamate subtype 5 receptors are quantified in the human brain with a novel radioligand for PET. *J Nucl Med* 49:2042-2048.
112. Pike VW. (2009) PET radiotracers: crossing the blood-brain barrier and surviving metabolism. *Trends Pharmacol Sci* 30:431-440.
113. Syvanen S, Lindhe O, Palner M, Kornum BR, Rahman O, Langstrom B, Knudsen GM, Hammarlund-Udenaes M. (2009) Species differences in blood-brain barrier transport of three positron emission tomography radioligands with emphasis on P-glycoprotein transport. *Drug Metab Dispos* 37:635-643.
114. Cymerman U, Pazos A, Palacios JM. (1986) Evidence for species differences in 'peripheral' benzodiazepine receptors: an autoradiographic study. *Neurosci Lett* 66:153-158.
115. Balaban RS, Hampshire VA. (2001) Challenges in small animal noninvasive imaging. *ILAR J* 42:248-262.
116. Kannan P, John C, Zoghbi SS, Halldin C, Gottesman MM, Innis RB, Hall MD. (2009) Imaging the function of P-glycoprotein with radiotracers: pharmacokinetics and in vivo applications. *Clin Pharmacol Ther* 86:368-377.
117. Guo Q, Brady M, Gunn RN. (2009) A Biomathematical Modeling Approach to Central Nervous System Radioligand Discovery and Development. *J Nucl Med* 50:1715-1723
118. Keller M, Montgomery S, Ball W, Morrison M, Snavely D, Liu G, Hargreaves R, Hietala J, Lines C, Beebe K, Reines S. (2006) Lack of efficacy of the substance P (neurokinin1 receptor) antagonist aprepitant in the treatment of major depressive disorder. *Biol Psychiatry* 59:216-223.
119. Lockhart A. (2006) Imaging Alzheimer's disease pathology: one target, many ligands. *Drug Discov Today* 11:1093-1099.

120. Feinendegen LE, Pollycove M. (2001) Biologic responses to low doses of ionizing radiation: detriment versus hormesis. Part 1. Dose responses of cells and tissues. *J Nucl Med* 42:17N-27N.
121. Volkow ND, Gillespie H, Mullani N, Tancredi L, Grant C, Ivanovic M, Hollister L. (1991) Cerebellar metabolic activation by delta-9-tetrahydro-cannabinol in human brain: a study with positron emission tomography and ^{18}F-2-fluoro-2-deoxyglucose. *Psychiatry Res* 40:69-78.
122. Mathew RJ, Wilson WH, Turkington TG, Coleman RE. (1998) Cerebellar activity and disturbed time sense after THC. *Brain Res* 797:183-189.
123. O'Leary DS, Block RI, Turner BM, Koeppel J, Magnotta VA, Ponto LB, Watkins GL, Hichwa RD, Andreasen NC. (2003) Marijuana alters the human cerebellar clock. *Neuroreport* 14:1145-1151.
124. Charalambous A, Marciniak G, Shiue CY, Dewey SL, Schlyer DJ, Wolf AP, Makriyannis A. (1991) PET studies in the primate brain and biodistribution in mice using (-)-5'-^{18}F-Δ^8-THC. *Pharmacol Biochem Behav* 40:503-507.
125. Gatley SJ, Lan R, Volkow ND, Pappas N, King P, Wong CT, Gifford AN, Pyatt B, Dewey SL, Makriyannis A. (1998) Imaging the brain marijuana receptor: development of a radioligand that binds to cannabinoid CB_1 receptors *in vivo*. *J Neurochem* 70:417-423.
126. Berding G, Muller-Vahl K, Schneider U, Gielow P, Fitschen J, Stuhrmann M, Harke H, Buchert R, Donnerstag F, Hofmann M, Knoop BO, Brooks DJ, Emrich HM, Knapp WH. (2004) [^{123}I]AM281 single-photon emission computed tomography imaging of central cannabinoid CB_1 receptors before and after Delta^9-tetrahydrocannabinol therapy and whole-body scanning for assessment of radiation dose in tourette patients. *Biol Psychiatry* 55:904-915.
127. Berding G, Schneider U, Gielow P, Buchert R, Donnerstag F, Brandau W, Knapp WH, Emrich HM, Muller-Vahl K. (2006) Feasibility of central cannabinoid CB_1 receptor imaging with [^{124}I]AM281 PET demonstrated in a schizophrenic patient. *Psychiatry Res* 147:249-256.
128. Li Z, Gifford A, Liu Q, Thotapally R, Ding YS, Makriyannis A, Gatley SJ. (2005) Candidate PET radioligands for cannabinoid CB_1 receptors: [^{18}F]AM5144 and related pyrazole compounds. *Nucl Med Biol* 32:361-366.
129. Mathews WB, Scheffel U, Rauseo PA, Ravert HT, Frank RA, Ellames GJ, Herbert JM, Barth F, Rinaldi-Carmona M, Dannals RF. (2002) Carbon-11 labeled radioligands for imaging brain cannabinoid receptors. *Nucl Med Biol* 29:671-677.
130. Horti AG, Fan H, Kuwabara H, Hilton J, Ravert HT, Holt DP, Alexander M, Kumar A, Rahmim A, Scheffel U, Wong DF, Dannals RF. (2006) ^{11}C-JHU75528: a radiotracer for PET imaging of CB_1 cannabinoid receptors. *J Nucl Med* 47:1689-1696.
131. Wong DF, Kuwabara H, Horti AG, Kumar A, Brasic J, Ye W, Alexander M, Hilton J, Williams V, Roberson M, Ravert H, Dannals R. (2008) Imaging of Human Cannaboid CB_1 Type Human Receptors with [^{11}C]OMAR. *J Nucl Med* 49(Suppl 1):131P.
132. Wong DF, Kuwabara H, Horti A, Kumar A, Brasic J, Ye W, Alexander M, Raymont V, Galecki J, Charlotte M, Cascella N. (2008) PET Imaging of cannabinoid CB_1 type receptors in healthy humans and patients with schizophrenia using [^{11}C]OMAR. *NeuroImage* 41(Suppl 2):O38.

133. Fan H, Kotsikorou E, Hoffman AF, Ravert HT, Holt D, Hurst DP, Lupica CR, Reggio PH, Dannals RF, Horti AG. (2009) Analogs of JHU75528, a PET ligand for imaging of cerebral cannabinoid receptors (CB_1): development of ligands with optimized lipophilicity and binding affinity. *Eur J Med Chem* 44:593-608.
134. Liu P, Lin LS, Hamill TG, Jewell JP, Lanza TJ, Jr., Gibson RE, Krause SM, Ryan C, Eng W, Sanabria S, Tong X, Wang J, Levorse DA, Owens KA, Fong TM, Shen CP, Lao J, Kumar S, Yin W, Payack JF, Springfield SA, Hargreaves R, Burns HD, Goulet MT, Hagmann WK. (2007) Discovery of N-{(1S,2S)-2-(3-cyanophenyl)- 3-[4-(2-[^{18}F]fluoroethoxy)phenyl]-1-methylpropyl}- 2-methyl-2-[(5-methylpyridin-2-yl)oxy]propanamide, a cannabinoid-1 receptor positron emission tomography tracer suitable for clinical use. *J Med Chem* 50:3427-3430.
135. Burns HD, Van Laere K, Sanabria-Bohorquez S, Hamill TG, Bormans G, Eng WS, Gibson R, Ryan C, Connolly B, Patel S, Krause S, Vanko A, Van Hecken A, Dupont P, De Lepeleire I, Rothenberg P, Stoch SA, Cote J, Hagmann WK, Jewell JP, Lin LS, Liu P, Goulet MT, Gottesdiener K, Wagner JA, de Hoon J, Mortelmans L, Fong TM, Hargreaves RJ. (2007) [^{18}F]MK-9470, a positron emission tomography (PET) tracer for *in vivo* human PET brain imaging of the cannabinoid-1 receptor. *Proc Natl Acad Sci U S A* 104:9800-9805.
136. Koeppe RA, Frey KA, Snyder SE, Meyer P, Kilbourn MR, Kuhl DE. (1999) Kinetic modeling of N-[^{11}C]methylpiperidin-4-yl propionate: alternatives for analysis of an irreversible positron emission tomography trace for measurement of acetylcholinesterase activity in human brain. *J Cereb Blood Flow Metab* 19:1150-1163.
137. Addy C, Wright H, Van Laere K, Gantz I, Erondu N, Musser BJ, Lu K, Yuan J, Sanabria-Bohorquez SM, Stoch A, Stevens C, Fong TM, De Lepeleire I, Cilissen C, Cote J, Rosko K, Gendrano IN, 3rd, Nguyen AM, Gumbiner B, Rothenberg P, de Hoon J, Bormans G, Depre M, Eng WS, Ravussin E, Klein S, Blundell J, Herman GA, Burns HD, Hargreaves RJ, Wagner J, Gottesdiener K, Amatruda JM, Heymsfield SB. (2008) The acyclic CB1R inverse agonist taranabant mediates weight loss by increasing energy expenditure and decreasing caloric intake. *Cell Metab* 7:68-78.
138. Goffin K, Bormans G, Casteels C, Bosier B, Lambert DM, Grachev ID, Van Paesschen W, Van Laere K. (2008) An in vivo [^{18}F]MK-9470 microPET study of type 1 cannabinoid receptor binding in Wistar rats after chronic administration of valproate and levetiracetam. *Neuropharmacology* 54:1103-1106.
139. Van Laere K, Goffin K, Casteels C, Dupont P, Mortelmans L, de Hoon J, Bormans G. (2008) Gender-dependent increases with healthy aging of the human cerebral cannabinoid-type 1 receptor binding using [^{18}F]MK-9470 PET. *NeuroImage* 39:1533-1541.
140. Van Laere K, Goffin K, Bormans G, Casteels C, Mortelmans L, de Hoon J, Grachev I, Vandenbulcke M, Pieters G. (2009) Relationship of type 1 cannabinoid receptor availability in the human brain to novelty-seeking temperament. *Arch Gen Psychiatry* 66:196-204.
141. Yasuno F, Brown AK, Zoghbi SS, Krushinski JH, Chernet E, Tauscher J, Schaus JM, Phebus LA, Chesterfield AK, Felder CC, Gladding RL, Hong J, Halldin C, Pike VW, Innis RB. (2008) The PET radioligand [^{11}C]MePPEP binds reversibly and with high specific signal to

cannabinoid CB_1 receptors in nonhuman primate brain. *Neuropsychopharmacology* 33:259-269.

142. Donohue SR. (2008) Development of Cannabinoid Subtype-1 (CB1) Receptor Ligands for PET. In: *Thesis for doctoral degree Department of Clinical Neuroscience*, Stockholm: Karolinska Institutet.
143. Fride E, Mechoulam R. (1993) Pharmacological activity of the cannabinoid receptor agonist, anandamide, a brain constituent. *Eur J Pharmacol* 231:313-314.
144. Abadji V, Lin S, Taha G, Griffin G, Stevenson LA, Pertwee RG, Makriyannis A. (1994) (*R*)-methanandamide: a chiral novel anandamide possessing higher potency and metabolic stability. *J Med Chem* 37:1889-1893.
145. McGregor IS, Issakidis CN, Prior G. (1996) Aversive effects of the synthetic cannabinoid CP 55,940 in rats. *Pharmacol Biochem Behav* 53:657-664.
146. Seidel J, Vaquero JJ, Green MV. (2003) Resolution uniformity and sensitivity of the NIH ATLAS small animal PET scanner: comparison to simulated LSO scanners without depth-of-interaction capability. *IEEE Trans. Nucl. Sci.* 50:1347-1350.
147. Liow J, Seidel J, Johnson CA, Toyama H, Green MV, Innis RB. (2003) A single slice rebinning/2D exact positioning OSEM reconstruction for the NIH ATLAS small animal PET scanner. *J. Nucl. Med.* 44:163P.
148. Johnson CA, Seidel J, Vaquero JJ, Pascau J, Desco M, Green MV. (2002) Exact positioning for OSEM reconstructions on the ATLAS depth-of-interaction small animal scanner. *Mol. Imaging Biol.* 4:S22.
149. Paxinos G, Watson C. (1998) *The rat brain in stereotaxic coordinates*. San Diego: Academic Press.
150. Paxinos G, Franklin KBJ. (2001) *The mouse brain in stereotaxic coordinates*. San Diego: Academic Press.
151. Tzourio-Mazoyer N, Landeau B, Papathanassiou D, Crivello F, Etard O, Delcroix N, Mazoyer B, Joliot M. (2002) Automated anatomical labeling of activations in SPM using a macroscopic anatomical parcellation of the MNI MRI single-subject brain. *NeuroImage* 15:273-289.
152. Imaizumi M, Kim HJ, Zoghbi SS, Briard E, Hong J, Musachio JL, Ruetzler C, Chuang DM, Pike VW, Innis RB, Fujita M. (2007) PET imaging with [^{11}C]PBR28 can localize and quantify upregulated peripheral benzodiazepine receptors associated with cerebral ischemia in rat. *Neurosci Lett* 411:200-205.
153. Hawkins RA, Phelps ME, Huang S-C. (1986) Effects of temporal sampling, glucose metabolic rates, and disruptions of the blood-brain barrier on the FDG model with and without a vascular compartment: studies in human brain tumors with PET. *Journal Cerebral Blood Flow and Metabolism* 6:170-183.
154. Akaike H. (1974) A new look at the statistical model identification. *IEEE Trans. Automat. Contr.* AC19:716-723.
155. Fujita M, Imaizumi M, Zoghbi SS, Fujimura Y, Farris AG, Suhara T, Hong J, Pike VW, Innis RB. (2008) Kinetic analysis in healthy humans of a novel positron emission tomography radioligand to image the peripheral benzodiazepine receptor, a potential biomarker for inflammation. *NeuroImage* 40:43-52.
156. Carson RE, Huang SC, Green MV. (1986) Weighted integration method for local cerebral blood flow measurements with positron emission tomography. *J Cereb Blood Flow Metab* 6:245-258.

157. ICRP. (2002) *ICRP Publication 89: Basic anatomical and physiological data for use in radiological protection: reference values. A report of age- and gender-related differences in the anatomical and physiological characteristics of reference individuals*. Oxford, U.K.: Pergamon Press.
158. ICRP. (1979) *ICRP Publication 30 Part 1: Limits for Intakes of Radionuclides by Workers*. Oxford, U.K.: Pergamon Press.
159. Stabin MG, Sparks RB, Crowe E. (2005) OLINDA/EXM: the second-generation personal computer software for internal dose assessment in nuclear medicine. *J Nucl Med* 46:1023-1027.
160. Liow JS, Lu S, McCarron JA, Hong J, Musachio JL, Pike VW, Innis RB, Zoghbi SS. (2007) Effect of a P-glycoprotein inhibitor, Cyclosporin A, on the disposition in rodent brain and blood of the 5-HT_{1A} receptor radioligand, [^{11}C](*R*)-(-)-RWAY. *Synapse* 61:96-105.
161. Donohue SR, Krushinski JH, Pike VW, Chernet E, Phebus L, Chesterfield AK, Felder CC, Halldin C, Schaus JM. (2008) Synthesis, ex vivo evaluation, and radiolabeling of potent 1,5-diphenylpyrrolidin-2-one cannabinoid subtype-1 receptor ligands as candidates for in vivo imaging. *J Med Chem* 51:5833-5842.
162. Schou M, Halldin C, Sovago J, Pike VW, Hall H, Gulyas B, Mozley PD, Dobson D, Shchukin E, Innis RB, Farde L. (2004) PET evaluation of novel radiofluorinated reboxetine analogs as norepinephrine transporter probes in the monkey brain. *Synapse* 53:57-67.
163. Seneca N, Finnema SJ, Farde L, Gulyas B, Wikstrom HV, Halldin C, Innis RB. (2006) Effect of amphetamine on dopamine D_2 receptor binding in nonhuman primate brain: a comparison of the agonist radioligand [^{11}C]MNPA and antagonist [11C]raclopride. *Synapse* 59:260-269.
164. Hill MN, Miller GE, Ho WS, Gorzalka BB, Hillard CJ. (2008) Serum endocannabinoid content is altered in females with depressive disorders: a preliminary report. *Pharmacopsychiatry* 41:48-53.
165. Wyffels L, Muccioli GG, De Bruyne S, Moerman L, Sambre J, Lambert DM, De Vos F. (2009) Synthesis, in vitro and in vivo evaluation, and radiolabeling of aryl anandamide analogues as candidate radioligands for in vivo imaging of fatty acid amide hydrolase in the brain. *J Med Chem* 52:4613-4622.
166. Evens N, Muccioli GG, Houbrechts N, Lambert DM, Verbruggen AM, Van Laere K, Bormans GM. (2009) Synthesis and biological evaluation of carbon-11- and fluorine-18-labeled 2-oxoquinoline derivatives for type 2 cannabinoid receptor positron emission tomography imaging. *Nucl Med Biol* 36:455-465.